2018

Nicotinic Acetylcholine Receptor Dependent Effects of Nicotine on HEK293T and HBO Cells

James D. Larsen
Virginia Commonwealth University

2018

Nicotinic Acetylcholine Receptor Dependent Effects of Nicotine on HEK293T and HBO Cells

James D. Larsen
Virginia Commonwealth University, larsenjd2@mymail.vcu.edu

Nicotinic Acetylcholine Receptor Dependent Effects of Nicotine on HEK293T and HBO Cells

A thesis submitted in partial fulfillment for the requirements of the degree of Master of Science at Virginia Commonwealth University.

By

James Larsen
Bachelor of Arts, University of Virginia; 2014

Director: Vijay Lyall, Ph.D.
Associate Professor of Physiology and Biophysics

Virginia Commonwealth University
Richmond, Virginia
December, 2018

Acknowledgement

I would like to thank Dr. Vijay Lyall for all his time, effort, and patience as I completed this Master's Program. I would like to thank Dr. Jie Qian and Dr. Shohba Mummalaneni for their mentorship as well, through teaching protocols, aiding in data analysis, and ensuring I had the means to complete each challenge laid before me. I would also like to thank my mother, Amy Larsen, who supported me throughout this program. Without her endless support and love, I could have never gotten to this finish line.

Table of Contents

List of Tables……...…**i**

List of Figures……...……**ii**

List of Supplemental Figures……..…….**iii**

List of Abbreviations…….……...**iv**

Abstract……..…..…….……**v**

Introduction……1

Introduction to Taste……..……..……1

Tongue, Taste Bud Cells, and Taste Receptor Cells…...…….……1

Physiology of Taste…….….4

Salty Taste……7

Sour Taste……..……...……...…….8

Umami Taste……..……...……9

Sweet Taste……..……..10

Bitter Taste……..……...……10

Acetylcholine Receptors……..……..11

Muscarinic Acetylcholine Receptors……..……...11

Nicotinic Acetylcholine Receptors……12

Nicotine …….…….……...14

Health Concerns related to Nicotine……...……...15

Nicotine activates both a TRPM5-independent and dependent pathway …… ……16

Objective of this study……...……18

Materials & Methods…….……..19

Results……...……26

Discussion…….……55

Supplemental Figures……..61

Bibliography…….……69

Vita……...…….81

List of Tables

1. Primers used for qRT-PCR for Taste Receptors……..…….24

2. Primers used for qRT-PCR to detect the mRNA of nAChRs….…….…….25

List of Figures

1. Diagrammatic representation of a taste bud…….….3

2. Mammalian Taste Receptors……6

3. Shared Taste Transduction Pathway of Bitter, Sweet, and Umami Tastes……13

4. Health Concerns related to Nicotine……..17

5. Gel Electrophoresis after DNA amplification via RT-PCR……...27

6. Immunofluorescence of nAChR in HEK293T Cells…….31

7. Double-Immunofluorescence nAChR subunits and TRPM5 in HEK293T Cells…….33

8. HEK293T cells loaded with Fura-2 at 340 (nm) and 380 (nm)…….36

9. Ca^{2+} measurement in HEK293T Cells……...38

10. Ca^{2+} measurement in HEK293T Cells in the presence of TRPM5 Blocker……41

11. qRT-PCR for nAChR subunit mRNA expression……...44

12. qRT-PCR for T2R38 mRNA expression…….48

13. The effect of Nicotine on nAChR subunit protein expression in HEK293T Cells……..50

14. Effect of Nic on BDNF synthesis and release in HEK293T cells……...53

List of Supplemental Figures

1. Expression of nAChR subunits, taste receptors, and intracellular signaling intermediates in HBO…….…….…….…….....62

2. Immunofluorescence staining of α5 in HBO cells…….……..……..63

3. Co-localization of α and B subunits in HBO cells and Co-localization of α5 subunit with TRPM5 in HBO cells …….……..…64

4. Effect of Nicotine and mecamylamine on temporal changes in [Ca2+]i in individual HBO cells …….…….……..65

5. Effect of Nicotine exposure on the nAChR subunit mRNA expression level in HBO cells 66

6. Effect of Nicotine and on α6 protein expression in HBO cells ……..….67

7. Effect of Nicotine on BDNF synthesis and release in HBO cells …….68

List of Abbreviations

Chorda Tympani Nerve……...……CT

Cranial Nerve……...CN

Cultured Human Fungiform Taste Cells……...……HBO

Endoplasmic reticulum…….ER

Amiloride Sensitive Epithelial Sodium Channel……...…..……ENaC

G Protein Coupled Receptor……GPCR

Human Embryonic Kidney Cells……...……HEK293T

Taste Receptor Cell……TRC

Taste Bud Cell……TBC

Transient Receptor Potential Variant 1……..……TRPV1

Acetylcholine Receptor……..…….AChR

Muscarinic Acetylcholine Receptor…….mAChR

Nicotinic Acetylcholine Receptor……..……nAChR

Transient receptor potential cation channel subfamily M member 5……....TRPM5

Brain Derived Neurotrophic Factor……BDNF

Mecamylamine……...Mec

Nicotine……...Nic

Abstract

NICOTINIC ACETYLCHOLINE RECEPTOR DEPENDENT EFFECTS OF NICOTINE ON HEK293T AND HBO CELLS

By James Larsen, B.A.

A thesis submitted in partial fulfillment for the requirements of the degree of Master of Science at Virginia Commonwealth University.

Virginia Commonwealth University, 2018

Director: Vijay Lyall, Ph.D., Assistant Professor, Department of Physiology

T2R receptors are the classical bitter taste receptors which detect and transduce bitter taste in a subset of taste receptor cells (TRCs). The TRPM5-dependent T2Rs are G-protein coupled receptors (GPCRs) and are linked to G protein, gustducin to initiate an intracellular signaling cascade for the transduction of bitter tastants. Nicotine is bitter. However, at present the transduction mechanisms for the detection of nicotine in are poorly understood. Previous studies from our laboratory using TRPM5 knockout (KO) mice demonstrated that the T2R pathway is insufficient in explaining the taste perception of nicotine. TRPM5 KO mice elicited chorda tympani (CT) taste nerve responses to nicotine, albeit significantly smaller than the wild type (WT) mice and still responded to nicotine as an aversive stimulus. Following addition of mecamylamine (Mec), a non-specific blocker of neuronal nicotinic acetylcholine receptors (nAChRs), CT responses to nicotine were partially inhibited in both WT and TRPM5 KO mice. Mec also decreases the aversive response to nicotine in both WT and TRPM5 KO mice. These studies led to the hypothesis that both a TRPM5-independent and TRPM5-dependent pathways are responsible for the detection and transduction of the bitter taste of nicotine in TRCs. The TRPM5-independent pathway most likely utilizes the nAChRs expressed in TRCs and function as bitter taste receptors for nicotine. We have subsequently demonstrated the expression of nAChRs in a subset of TRPM5-positive TRCs. However, this mechanism is not well understood in other cell

types, particularly undifferentiated epithelial cells, such as HEK293T cells. The specific aims of this project were: (i) To identify which components of T2R-dependent taste reception as well as components of nAChRs are expressed in HEK293T cells; (ii) To determine if HEK293T cells co-express these components; (iii) To identify if exposure to nicotine modulates the expression of T2R and nAChR dependent components in HEK293T cells; (iv) To determine if TRCs express functional nAChR ion channels; and (v) To determine if nAChRs are involved in the release of neuropeptides, such as brain-derived neurotrophic factor (BDNF) in HEK293T cells. The data obtained in HEK293T cells was compared with parallel studies on adult cultured human fungiform taste cells (HBO) done independently by Dr. Jie Qian, a postdoctoral fellow in Dr. Vijay Lyall's lab. The results of combined studies on HBO and HEK293T cells indicates that TRPM5-positive cells also co-express ionotropic nAChRs, comprising α and β subunits. The nAChRs are capable of forming ion pores and when stimulated by nicotine and create a parallel TRPM5-independent pathway for the detection of nicotine. Using molecular and immunocytochemical techniques, our results demonstrate that mRNAs and proteins for bitter taste receptors and downstream intracellular signaling components as well as subunits necessary for the formation of nAChRs are expressed in HBO and HEK293T cells. Results demonstrated that TRPM5-positive HEK293T cells co-expressed nAChR subunits throughout the entire population. Nicotine increased the influx of Ca^{2+} in a dose dependent manner, which was somewhat reduced by the addition of TRPM5 blocker, triphenylphosphine oxide (TPPO). Both mRNA and protein expression were altered in a biphasic pattern with a maximum increased observed at 0.5 μM nicotine with a decrease in expression at higher concentrations. The synthesis of neurotrophic factor BDNF, required for maturation of taste bud cells and their innervating nerves, increased in HEK293T cells exposed to nicotine, however, nicotine did not trigger the release of BDNF. These results were then compared

and contrasted with HBO cells to better understand the comparative effects of nicotine on both undifferentiated and differentiated cells. The data on HBO cells is presented in the Appendix.

Chapter 1: Introduction

1.1 Introduction to Taste

Taste or gustation is one of five traditional senses organisms have evolved in order to aid in survival alongside sight, touch, hearing, and olfaction. Humans can distinguish between five primary taste qualities: bitter, sweet, umami, salty, and sour (21). Together these taste qualities aid organisms in obtaining adequate nutrients and energy while avoiding toxic substances (18, 21).

The taste quality of objects consumed are determined as dissolved molecules and ions, referred to as tastants, stimulate taste receptor cells (TRCs) found in taste buds (47). Bitter tastants are aversive and serve as a protective mechanism against toxic substances such as q uinine, plant alkaloids, many non-Na^+ mineral salts, alcohol, and nicotine (47). Sweet tastants signify high energy compounds such as carbohydrates. Umami taste is elicited by L-amino acids, such as L-glutamate (MSG), indicating protein content and defined by a savory taste (52). Salty stimuli include NaCl and other mineral salts and are often produced through the influx of Na^+ across the apical membrane of a subset of taste receptor cells. Salty taste aids in maintaining electrolyte homeostasis through water retention and expulsion as well as maintaining blood volume (47). Sour tastants, like bitter tastants, serve as aversive stimuli to avoid mineral and organic acids, preventing ad libitum ingestion of acids and maintaining proper acid-base balance (47). The threshold of tastant concentrations differs between individuals and is genetically determined, likely playing a role in individual food preferences (11).

1.2 Tongue, Taste Bud Cells, and Taste Receptor Cells (TRCs)

The tongue is the major organ of the gustatory system, comprised of a sophisticated structure including epithelial, neural, connective, and vascular tissues. The tongue acts as a detector for both nutrients and toxins entering the body, sending information to the brain to prepare

downstream organ systems for nutrient absorption and other metabolic functions. The dorsal surface of the tongue is characterized as stratified squamous epithelium with mucosal projections known as lingual papillae, which house the taste buds and their TRCs and give the tongue its characteristic rough texture (2). The lingual papillae are made up of four subtypes, the filiform, fungiform, foliate, and circumvallate papillae (2). Filiform papillae are located across the majority of the tongue and lack taste buds. Fungiform papillae are located in the apical tip and lateral edges of the tongue and form mushroom-shaped structures. Foliate papillae are located on the posterior-lateral portions of the tongue (2). Circumvallate papillae are located at the most posterior portion of the tongue and form an inverted 'V' shape structure (2).

Taste buds are formed through clustered groups of TRCs and vary in size from 50 to 150 TRCs (45, 2). The elongated TRCs come together to form the characteristic oval shape of a taste bud. Each TRC contains apical microvilli which house receptors for the detection of specific tastants within the oral cavity. In order to achieve taste perception various Cranial Nerves (CN) innervate these TRCs for communication from the taste sensing gustatory system to the brain. The anterior two thirds of the tongue is innervated by the Chorda Tympani branch of the facial nerve (CN VII) while the posterior third is innervated by the lingual-tonsillar branch of the glossopharyngeal nerve (CN IX) (2). The trigeminal nerve (CN V) and the vagus nerve (CN X) also assist in the transduction of taste (2).

These specialized TRCs respond to various taste stimuli by cell depolarization, increase in intracellular Ca^{2+} concentrations ($[Ca^{2+}]_i$) and release of taste-specific neurotransmitter, Adenosine Triphosphate (ATP) (20).

1

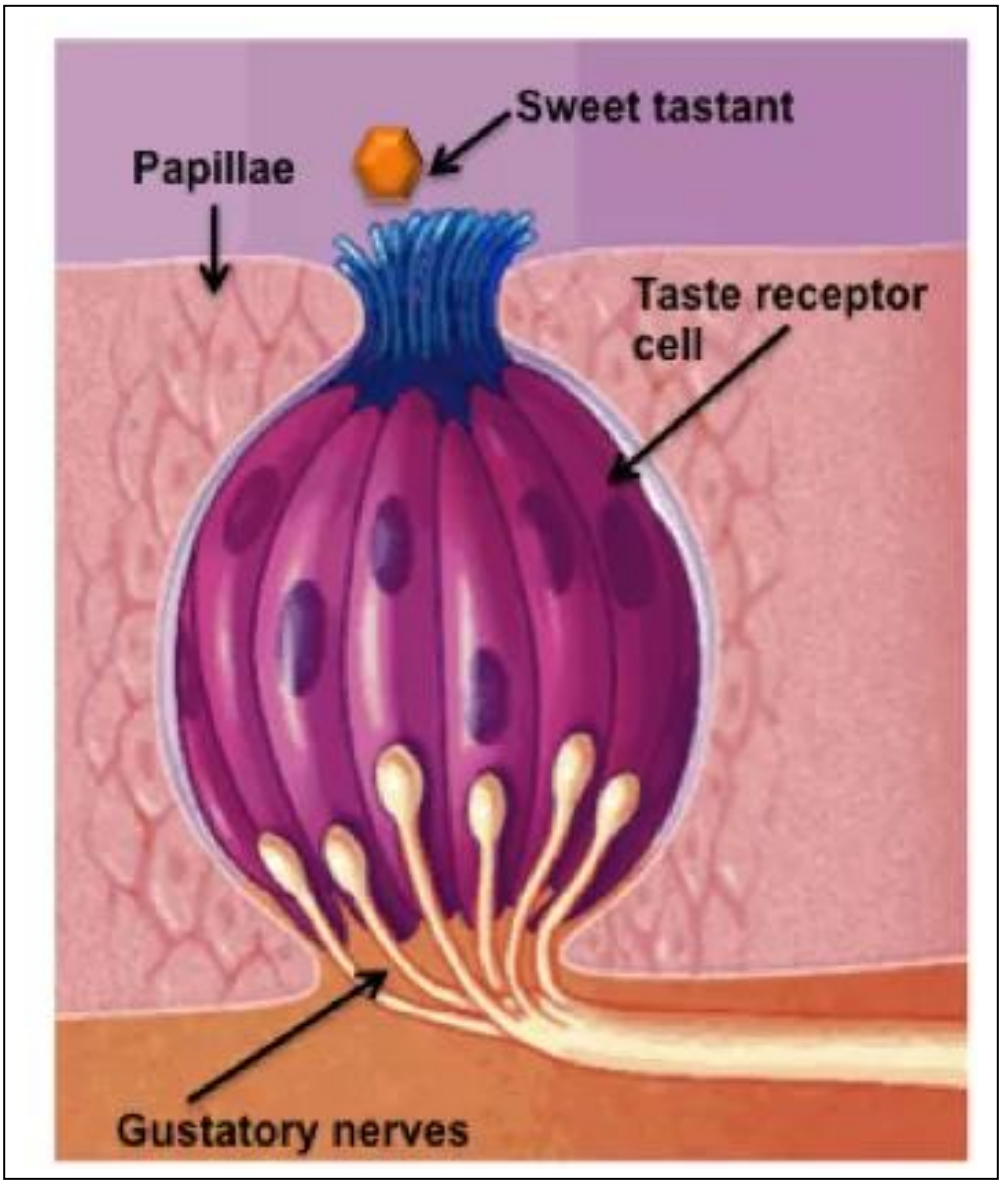

Figure 1. Diagrammatic representation of a taste bud: This diagram illustrates the structure of a taste bud; elongated taste receptor cells containing receptors specific for different taste qualities (in this example a sweet tastant is used). Taste cells are innervated by gustatory nerve fibers (13).

Stimuli representing each of the five taste qualities are detected by specific taste receptors. Each taste receptor is only present on a specific subset of TBCs. Receptor binding initiates a cascade of downstream transducing mechanisms (44). Umami, bitter, and sweet taste receptors are G-protein coupled receptors (GPCRs) and are coupled with gustducin which begin a process to release internal Ca^{2+} from the endoplasmic reticulum (ER), eventually leading to the release of ATP (20). Sour taste receptors are H^+ proton channels. Salty taste receptors are Na^+-sensing ion channels. For sour and salty tastes, entry of H^+ and Na^+ depolarizes the taste cell, activating voltage-gated Ca^{2+} channels, allowing entry of external Ca^{2+} into the cell to trigger release of the taste-specific neurotransmitter, ATP (20).

1.3 Physiology of Taste

Through DNA sequencing, a multigene family of GPCRs involved in the transduction of bitter, sweet, and umami taste stimuli was discovered (11). The canonical taste receptors are divided into taste receptor type 1 (T1R) and taste receptor type 2 (T2R) GPCR families, and further differentiated through member numbers of each receptor type (11, 9). The T1R family of GPCRs consists of T1R1, T1R2, and T1R3, which form heterodimers to create functional taste receptors (11). Umami taste utilizes a heterodimer of T1R1 and T1R3 to detect stimuli containing L-amino acids, indicating protein content and defined by a savory taste. Sweet taste utilizes the T1R2 and T1R3 heterodimer to detect stimuli containing high levels of sugars, carbohydrates, sweet proteins and artificial sweeteners (11). T1R3 KO mice have been demonstrated to display residual responses to both umami and sweet stimuli. This indicates that, in addition to GPCRs, other taste receptors are involved in the detection of sweet and umami stimuli (11).

The T2R family of GPCRs is utilized for bitter taste reception and transduction. The signaling pathways for these GPCRs are shared as gustducin is activated post stimulation through receptor specific tastants (9).

Salty tastant detection involves both a Na^+-specific and cation non-selective pathway.. The Na^+-specific pathway involves Na^+ influx via amiloride-sensitive epithelial sodium channels (ENaC) expressed in a subset of fungiform TRCs. A candidate cation non-specific cation channel TRPV1 has been proposed as a pathway for amiloride-insensitive salt responses in rodents (15). Finally, sour taste transduction is mediated through the PKD2L1 ion channel although other Zn^{2+}-sensitive proton channels may also be involved (11,15).

The bitter, sweet, and umami taste transduction pathways are all triggered through an interaction between specific tastants for each taste quality and a seven transmembrane domain GPCR. While each receptor representing its given taste quality varies between the three taste domains, the downstream signaling cascade is shared between the three, focusing on increasing internal Ca^{2+}, activating non-selective cation channel TRPM5 (Transient receptor potential cation channel subfamily M member 5) to depolarize the cell, and finally release of neurotransmitter in the form of ATP (20). After a bitter, sweet, or umami tastant binds to its specific receptor on a TRC, GPCRs activate heterotrimeric G_α-gustducin and its βγ partners Gβ1 and γ13. The βγ subunit then interacts with phospholipase Cβ2 (PLCβ2) converting PIP_2 to IP_3 and DAG. IP_3 acts as a second messenger, interacting with IP_3R_3 ion channels along the ER and causing them to open, releasing internal Ca^{2+} (20). This influx of Ca^{2+} then targets non-selective cation channel TRPM5 and gap junction hemi-channel Panx1 (20). As TRPM5 opens, Na^+ freely enters the cell down the concentration gradient, depolarizing the cell and triggering the secretion of neurotransmitter ATP through the hemi-channel

2

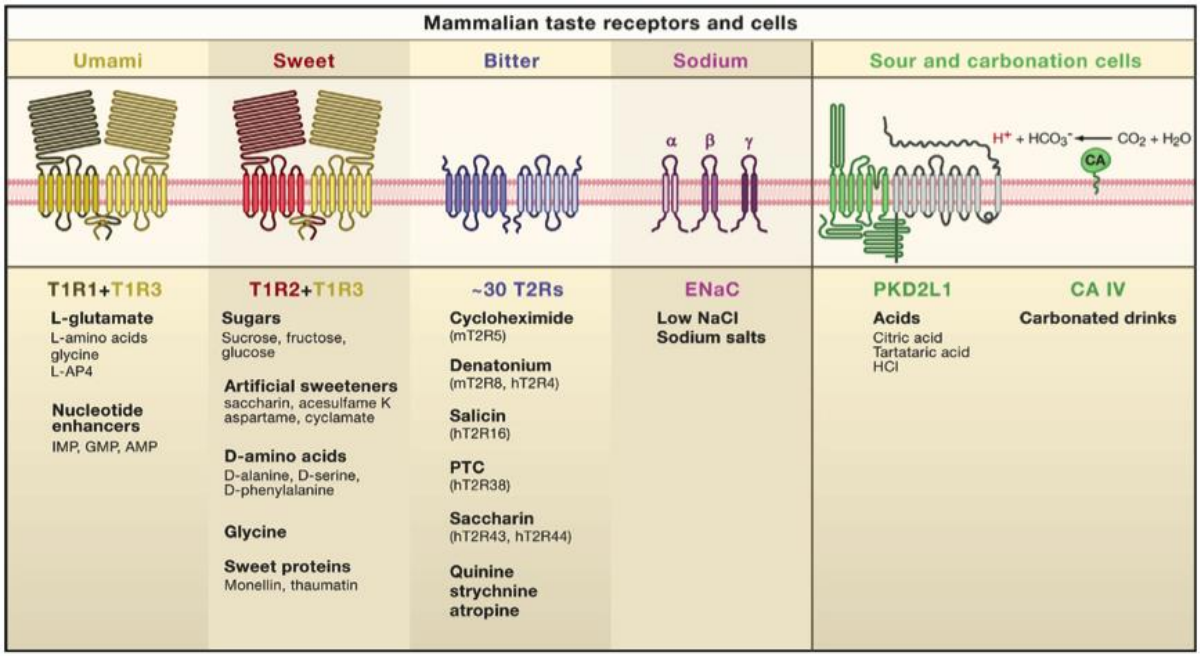

Figure 2. Mammalian Taste Receptors: This diagram illustrates taste receptors representing the five taste qualities, and examples of taste stimuli that activate them (51)

Panx1 and into the extracellular space (20). KO mice demonstrated to lack TRPM5 have been shown to lack the ability to sense bitter, sweet, and umami taste senses through both behavioral studies as well as through chorda tympani response recordings. ATP was confirmed as the relevant neurotransmitter as KO mice lacking the ATP-sensing P2X ligand-gated ion channels demonstrated no neural responses in chorda tympani and glossopharyngeal taste nerves to these specific tastants (20).

1.3.1 Salty Taste

Salty taste reception is used to identify the nutrient and mineral concentration of food in order to maintain ion and water homeostasis in the body. The major tastant of this taste quality is Na^+ (24). The Na^+-specific taste pathway is inhibited through application of amiloride to the anterior tongue (16). Salty tastant reception is transduced through both an amiloride-sensitive and a amiloride-insensitive pathway which act as Na^+-sensitive and insensitive pathways respectively. The amiloride-sensitive pathway primarily functions via the amiloride-sensitive epithelial sodium channels, ENaC. α-ENaC conditional KO mice lacking α-ENaC only in the taste cells have been shown to lick NaCl solutions at a reduced rate, signifying a reduced appetitive response to salt, as well absence of amiloride-sensitive chorda tympani response to NaCl (15).

Humans, however, have been shown to primarily detect salty tastants through amiloride-insensitive pathways, as application of amiloride shows a greatly diminished effect on salty tastant perception in humans compared to mice. Unlike mice, humans express an additional ENaC subunit, δ-ENaC subunit. This is in addition to the α, β, and γ subunits expressed in both human and rodent epithelial tissues. The δ-subunit can form a δβγ complex in place of the α-subunit which is approximately ten-fold less sensitive to amiloride than its αβγ counterpart (15). These results

suggest that while mice primarily perceive salty tastants through amiloride-sensitive pathways, humans rely more heavily on amiloride-insensitive pathways (15).

The suggested amiloride-insensitive pathway utilized by humans is hypothesized to be a nonspecific cation channel TRPV1 which is permeable to Na^+, K^+, NH_4^+, and Ca^{2+} which are all perceived as salty by humans (34). While the TRPV1 channel is not expressed in mice TRCs, it has been shown to be located within trigeminal nerve endings (34). TRPV1 has also been shown to elicit chorda tympani responses in the presence of NaCl and amiloride, while these responses are abolished in the presence of TRPV1 antagonists, SB-366791 and capsazepine (34). At this time, the signaling steps between TRPV1 channel activation and increase in Na^+ flux across taste receptor cell apical membrane are not known.

1.3.2 Sour Taste

The mechanism for sour taste was likely evolutionarily selected due to its ability to detect food which is spoiled or strongly acidic. Sour tastants are detected through ion channel PKD2L1 which is expressed in a subset of TRCs known as Type III cells (26). Through cell ablation, it has been demonstrated that ablation of Type III cells from taste buds lead to an abolished chorda tympani responses to sour taste stimuli (26). Different mechanisms of sour taste transduction are utilized based on the strength of the acid stimuli. Strong acids utilize Zn^{2+}-sensitive proton channels to allow the entry of H^+ into the cell whereas weak organic acids permeate apical cell membranes as neutral molecules and dissociate inside the cell to decrease taste receptor cell intracellular pH (pH_i) (33). In both situations, acid-induced decrease in pH_i is the proximate stimulus for sour taste transduction (33). As protons enter the cell, they interact with the K^+ channel, blocking these channels and preventing a resting efflux of K^+, leading to the depolarization of the cell and eventual generation of action potentials. (18, 27, 39).

CO_2 is also detected through the sour taste pathway through apical carbonic anhydrase 4 (CA4) which is co-expressed with cells containing PKD2L1 (26). It is likely that both extracellular and intracellular carbonic anhydrases are involved in CO_2 sensing.

1.3.3 Umami Taste

The term used to denote savory taste "umami" originated from the Japanese term for delicious, umai (32). Umami taste is classically considered to detect food which contain high levels of L-amino acids such as L-glutamate as well as ribonucleotides such as 5'-monophosphate (IMP) or guanosine-5'- monophophate (GMP) (28, 32). These tastants are considered to denote food with high protein content, giving the umami taste sensation its distinct savory characteristic (28, 31).

Several receptors have been discovered to bind with umami tastants including the T1R1/T1R3 GCPR heterodimer as well as a variant of the glutamate receptor-4 (mGluR4t), both of which are expressed at the apical membrane of taste cells (31, 28). Glutamate functions as neurotransmitter in many nerve cells, however these cells express their glutamate-sensitive receptors on the basolateral membrane, creating a distinct class of cells which respond to glutamate as a tastant compared to those that respond to glutamate as a neurotransmitter (28, 31).

Umami taste response through the T1R1/T1R3 heterodimer has been shown to be amplified through addition of IMP and GMP (53). T1R1 KO mice were compared to T1R1/T1R3 KO mice, where T1R1 KO mice showed a diminished but residual response to umami tastants and the T1R1/T1R3 KO mice demonstrated a completely abolished response to umami stimuli, leading to the conclusion that the mammalian umami receptor is a combination of both T1R1 and T1R3 (53). At present it is not clear if variant of the glutamate receptor-4 (mGluR4t) enhance glutamate response in the presence of IMP or GMP.

1.3.4 Sweet Taste

Sweet taste aids in the identification of edible material containing high-energy compounds in the forms of sugars and carbohydrates. Sweet taste transduction begins with the detection of sweet tastants through heterodimeric GPCR T1R2/T1R3 at the apical membrane of specific sweet TRCs (52). The receptor was identified through genetic mapping of rodent models, in which the mouse loci, Sac, was identified as the locus responsible for sensitivity to sweets such as sucrose and fructose (35). Human genes were then scanned until T1R3 was identified as a GCPR within an orthologous region to the mouse Sac (35). T1R3 was hypothesized as the sweet taste receptor until researchers observed that singular T1R3 was not enough to elicit sweet taste responses and that heterodimeric T1R2/T1R3 was required to yield functional sweet taste receptors (35, 52, 53).

1.3.5 Bitter Taste

Bitter taste is primarily used to identify natural toxins and alkaloids in edible materials. Mapping of DNA sequences identified the T2R (48) GPCR as the primary receptor for bitter tastants and are located in the circumvallate, foliate, and fungiform papillae (11, 38). The T2R family of receptors is encoded by 25-30 different genes. TRCs have been shown to express multiple T2R genes to increase the range of bitter tastants which can be identified (11, 38). Conditional T2R KO mice shown to lack T2R in their taste buds have been demonstrated to lack responses to bitter tastants, such as quinine, and can no longer distinguish between quinine and water in behavioral studies. The signaling pathway which follows tastant binding to T2R is the same as the other GPCR-dependent taste qualities, sweet and umami. Much like the umami pathway, the bitter taste utilizes gustducin as the G protein responsible for the previously stated activation of PLCβ2 through the βγ-gustducin subunit, whereas α-gustducin subunits activates

phosphodiesterase (PDE), decreasing cAMP levels to increase $[Ca^{2+}]_i$, and eventually releasing neurotransmitter ATP (11, 35, 48).

A specific T2R isoform in humans worth noting is the T2R38 isoform which affects the ability to detect both 6-n-propylthiouracil (PROP) and phenylthiocarbamide (PTC) (19). Sensitivity or insensitivity to these compounds has been demonstrated to effect the perceived bitterness of compounds including ethanol (19). It is hypothesized that a heterozygous population was evolutionarily desirable as it allows greater flexibility in bitter taste perception of the population as a whole (19). Polymorphisms in T2R38 have been hypothesized to protect individuals from the addictive qualities of both nicotine and alcohol as well (12).

1.4 Acetylcholine Receptors

Acetylcholine receptors (AChRs) are ligand-gated neurotransmitter receptors which bind acetylcholine and transmit the appropriate signal (3). There are two types of AChRs named for their major agonists, muscarinic AChRs (mAChRs) and nicotinic AChRs (nAChRs). Acetylcholine and acetylcholine receptors are also expressed in taste cells (56, 57).

1.4.1 Muscarinic Acetylcholine Receptors

There are five subtypes of mAChRs identified as M1 through M5. M1, M3, and M5 AChRs are G-coupled metabotropic receptors and are activated relatively slowly (milliseconds to seconds) before activating a G protein, resulting in a signaling cascade similar to that of the GPCR signaling cascades found in bitter, sweet, and umami taste pathways by activating phospholipase C (PLC), generating two secondary messengers, IP_3 and DAG and releasing $[Ca^{2+}]_i$ and act as excitatory receptors (3). M2 and M4 AChRs inhibit adenylyl cyclase causing a decrease in free cAMP as a second messenger and act as inhibitory receptors (3). All five subtypes are found within the CNS. M1AChRs are typically also found in secretory glands. M2 AChRs are found in cardiac tissue and

play a role in the closing of Ca^{2+} channels controlling both rate and force of contraction in the heart (3). M3 AChRs are found in smooth muscle and secretory glands. mAChRs are inhibited by a toxin from *Atropa belladonna* known as atropine (3).

1.4.2 Nicotinic Acetylcholine Receptors

nAChRs are ionotropic receptors and, upon binding with its ligand, undergo a conformational change, forming an ion pore which allows positive ions to freely flow through, typically Na^+ or K^+ ions, depolarizing the cell and releasing relevant neurotransmitters (3). Unlike mAChRs, the rate of signal transmission is much faster (microseconds) (3). While mAChRs are function through the parasympathetic nervous system (PSNS) receptors, nAChRs function within the both the PSNS and the sympathetic nervous system (SNS) (3). Muscle-type nAChRs are found in neuromuscular junctions whereas neuronal-type nAChRs are found in synapses between neurons and throughout the CNS. nAChRs are inhibited by a component of krait snake venom known as α-bungarotoxin (3).

Functional nAChRs are pentamers consisting of various α and β subunits arranged around a central pore (3). Each subunit consists of four major components: an extracellular NH_2-terminal domain, three transmembrane (TM) domains, a cytoplasmic loop of variable size and amino acid sequence, and a fourth TM domain containing an extracellular C-terminal sequence (3). This fourth TM domain is composed of β-strands that align in a configuration termed a β-barrel. There are currently ten known α subunits, identified as α1 through α10, as well as four β subunits, identified as β1 through β4 (3). A pentamer consisting of α4 and β2 subunits is the most common form found in the brain (42). The only subunit capable of creating homomeric pentamers is α7 (3).

3

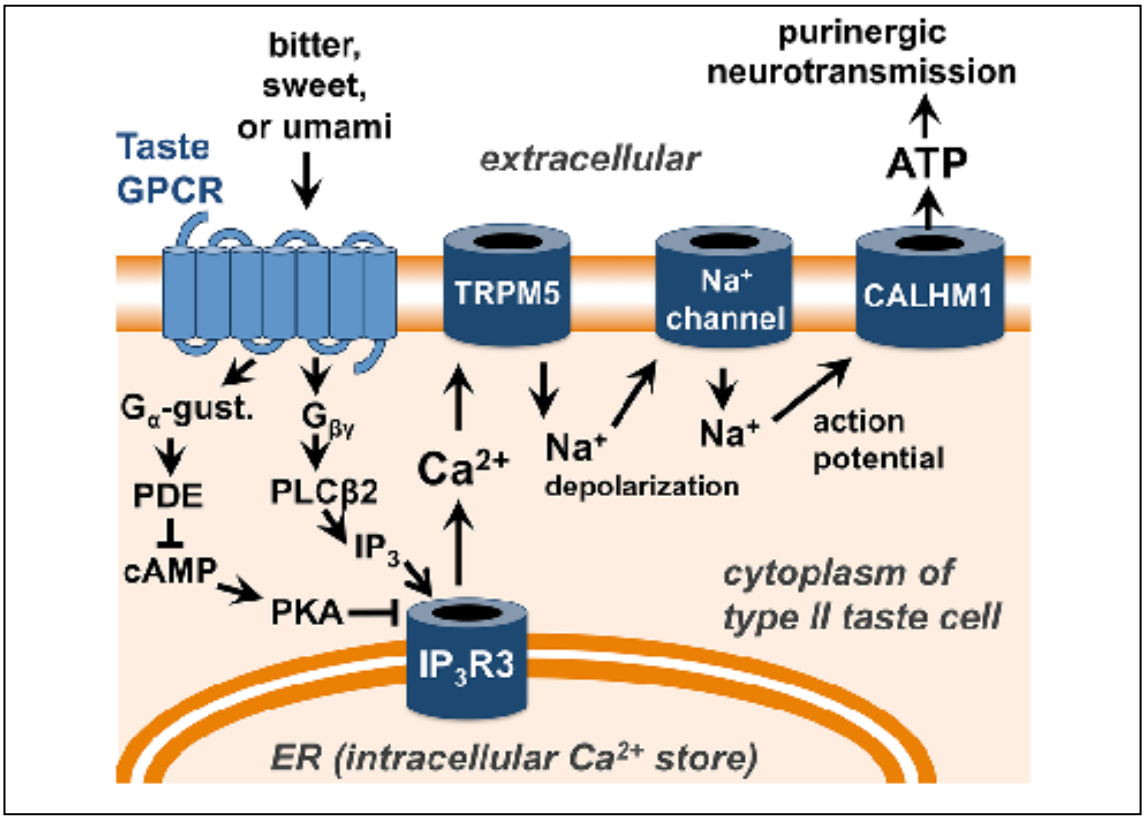

Figure 3. Shared Taste Transduction Pathway of Bitter, Sweet, and Umami Tastes: This diagram illustrates the transduction pathway following the binding of taste-specific ligand and subsequent activation of G Protein Gustducin (30).

Ligands bind to nAChRs in pockets formed between α subunits and the "back" face of an adjacent subunit (3). Upon binding, a rotational force is produced within the β-barrel, causing TM2 to rotate from a closed hydrophobic configuration to an open hydrophilic configuration which allows the flow of ions (3).

1.5 Nicotine

Nicotine is the principal alkaloid of tobacco, acting as a natural insecticide in tobacco leaves (5). Within a commercial grade cigarette, there is between 10 to 30 mg nicotine (5). Tobacco used within cigars contains between 15 to 40 mg nicotine (5). A gram of chewing tobacco contains 6 to 8 mg nicotine (5). A piece of nicotine gum contains 2 to 4 mg nicotine (5). A nicotine patch contains between 8 to 100 mg nicotine, variant upon desired strength (5). Popular vaping product Juul pods contain approximately 23 mg nicotine (1).

Nicotine in tobacco is primarily in the levorotary (*S*)-isomer and less than 1% nicotine content is (*R*)-nicotine (5). Nicotine is absorbed in the body through tar droplets which are inhaled through burning tobacco and its relative absorption rate is dependent on the pH at which it is absorbed. Nicotine is thought to be a weak base (pKa: 8.0) and in this state will not rapidly cross membranes (5). However, the pH of smoke from flue-cured tobacco found in most cigarettes is acidic, leading to a more rapid absorption (5). Once tobacco smoke reaches the lungs, nicotine is rapidly absorbed and blood concentrations rise (5). After a single puff, nicotine reaches the brain in about 10 to 20 seconds, leading to behavioral reinforcement (5). After smoking for 9 minutes, nicotine concentrations peak 30 minutes later (5). This peak concentration is approximately 15 ng/mL or 92 nM concentration nicotine in the blood for cigarettes, cigars, chewing tobacco, nicotine patches and vaping liquids and 10 ng/mL or 62 nM concentration nicotine in the blood for nicotine gum (5). These numbers can greatly vary, however, as smokers can manipulate their

dosage of nicotine based on the size of their puff. In the case of nicotine patches, nicotine is absorbed through the skin, where dosages and rate of release depend upon the permeability of the skin and the rate of passage through the membrane of the many products advertised as nicotine patches (5). All nicotine patches are believed to have an initial lag time of one hour before nicotine appears within the blood (5).

Nicotine is metabolized through the liver into a large number of metabolites, the most common of which is cotinine, making up between 70 to 80% of all nicotine metabolites (5).

1.6 Health Concerns Related to Nicotine

Tobacco, the primary source through which smokers intake nicotine, has been identified by the World Health Organization as the leading cause of preventable cancers in the world with approximately 1.27 billion tobacco users worldwide (36, 45). The Center for Disease Control and Prevention (CDC) estimates that over 16 million Americans live with a disease caused by nicotine intake and that worldwide over 6 million deaths are attributed to smoking and nicotine each year (8).

The ability of nicotine to stimulate reward centers in the brain, resulting in mood elevation and feelings of increased cognitive function, gives nicotine its initial addictive quality (36, 45). Chronic nicotine use can lead to a desensitization of GABAergic neurons which in part lose their ability to inhibit dopamine, reinforcing nicotine cravings (36).

Along with its highly addictive nature, nicotine is understood to adversely affect multiple organ systems including the heart, kidneys, and lungs (36). Stimulation of nAChRs by nicotine has been demonstrated to both initiate and progress cancers in the lungs, gastrointestinal system, pancreas, cardiovascular system, respiratory system, immunological system, ocular system, renal system, breasts, and both male and female reproductive systems through mechanisms which aid in

tumor formation and growth, activation of kinases which increase resistance to chemotherapy, increased rate of cancer metastasis, and a plethora of other symptoms (36). Secondhand smoke has been demonstrated as an agent of chronic obstructive pulmonary disease and lung cancer (36). Simply handling green tobacco leaves has been known to cause acute nicotine toxicity, leading to headache, nausea, vomiting, giddiness, loss of appetite, fatigue and tachyarrythmias (36).

1.7 Nicotine activates both a TRPM5-independent and dependent pathway

Oral detection and encoding of nicotine were once thought to be primarily carried out through the bitter taste receptors, T2R, as nicotine is an alkaloid compound. Furthermore, gustatory neurons have been demonstrated to discriminate between nicotine and other bitter tastants (40). TRPM5 KO mice have been shown to no longer sense quinine in solution with water but were able to identify nicotine as an aversive stimulus (40). TRPM5 KO mice were also shown to elicit a residual response to nicotine in chorda tympani recordings and this residual response was further diminished through the addition of non-selective nAChR blocker, mecamylamine (40). These results suggest that nicotine uses both a TRPM5-dependent and -independent pathway for detection and transduction of the bitter taste of nicotine through T2Rs and nAChRs respectively.

Human fungiform taste bud cells (HBO) have been shown to co-express nAChRs on TRPM5 positive cells, further supporting the hypothesis that both pathways work in unison in the transduction of nicotine (43).

4

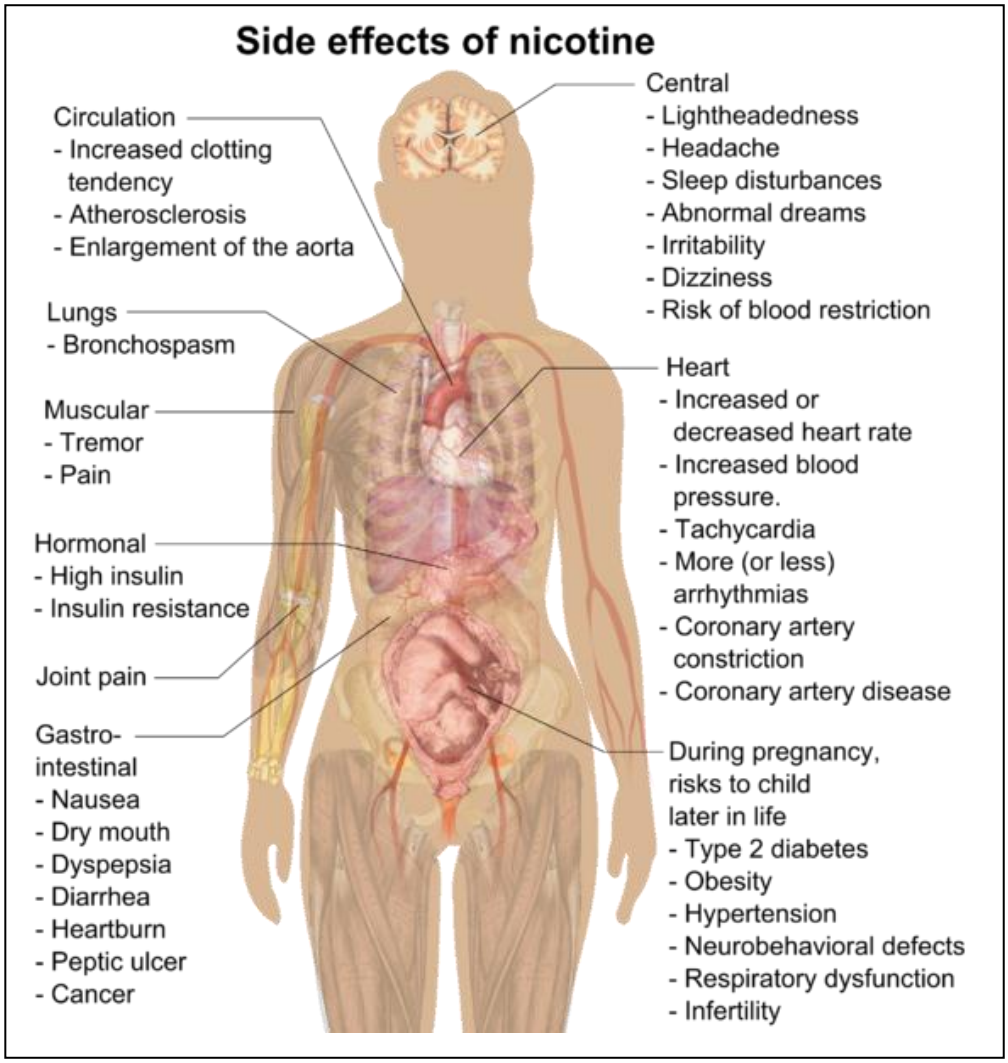

Figure 4. Health Concerns related to Nicotine: This diagram demonstrates many of the health consequences associated with nicotine absorption in the various muscles and organ systems of the body (50).

1.8 Objective of the Study

In humans, nicotine taste perception was once thought to be primarily regulated through bitter-tasting T2R receptors, however, evidence has shown that nAChRs play a parallel role as well. While both TRPM5-dependent and TRPM5-independent mechanisms are expressed in bitter sensing TRCs, the bitter taste of nicotine via T2Rs is TRPM5-dependent, whereas detection of the bitter taste of nicotine via nAChRs is TRPM5-independent (43). Nicotine has been demonstrated to produce a residual effect in the absence of the T2R pathway in TRPM5 KO mice and co-localization has been observed between TRPM5 and nAChR subunits in HBO cells (40). Currently, it is unknown if Human Embryonic Kidney (HEK293T) cells contain the functional receptors representing all of the five taste qualities and their downstream signaling components. In addition, it is not known if HEK293T cells express nAChRs other than α5 and α7. It is also not known if nicotine directly affects expression and function of T2Rs and nAChRs-and thereby taste perception and sensitivity to nicotine. It is also unknown how these changes in undifferentiated cells compares to those found in adult human fungiform (HBO) cells which contain all the receptors and signaling components associated with taste as well as nAChRs (43).

Both HEK293T and HBO cells are human cell lines however HEK293T, as embryonic and undifferentiated cells, will serve as a control against the differentiated HBO cells in order to identify the comparative expression and function of nAChRs in HEK293T and HBO cells. My hypothesis is that long term exposure to nicotine will modulate both T2R and nAChR subunit expression, exposure to nicotine in the presence of TRPM5 blocker will produce a residual response, and that TRPM5 positive cells will also co-express nAChR subunits similar to adult HBO studies. To test this hypothesis, we complete the following experiments: 1) RT-PCR to detect the presence of mRNA for taste receptors, their downstream components and nAChRs,

2)Immunostaining to determine which types of receptors are present in each cell type as well as which cells co-express these receptors, 3)calcium imaging to understand the function of the nAChRs, 4)qRT-PCR to determine quantifiable changes in mRNA expression in response to nicotine, 5)Western Blot to determine how changes in mRNA expression correlate to changes in protein expression, and finally 6)ELISA to determine the contribution of nAChRs in the release of Brain-Derived Neurotrophic factor (BDNF) in each cell line.

The pursuit to identify mechanisms by which the bitter taste of nicotine is transduced could have a profound effect on formulating preventative measures which could be taken towards reducing nicotine addiction.

Chapter 2: Materials & Methods

2.1 Human Embryonic Kidney Cell (HEK293T)

HEK293T cells are human embryonic kidney cells obtained from (American Type Culture Collection, Manassas, VA). HEK293T cells were cultured in Dulbecco's Modified Eagle's Medium (DMEM) (VWR Life Science) supplemented with 10% Fetal Bovine Serum (FBS) (Hyclone, Logan, UT), 4-(2-hydroxyethly)-1-piperazineethanesulfonic acid (HEPES), and Penicillin-Streptomycin (Invitrogen, Carlsbad, CA) at 37 °C in 95% O_2/5% CO_2.

These HEK293T cells will act as a control in comparison against HBO cells as both are human cell lines. HEK293T cells have been previously demonstrated to express nAChR subunits α5 and α7 (81). Adult human kidney cells have also been shown to express both the α7 subunit and T2R receptors, similar to HBO cells as well (43, 73).

2.2 Western Blots to detect the expression of nAChR and taste receptor proteins in HEK293T Cells

HEK293T cells were treated with 0.1 μM, 0.25 μM, 0.5 μM, and 1.0 μM nicotine in the culture medium for 24 h at 37 °C in 95% O_2/5% CO_2. Untreated HEK293T cells were used as ~~a~~ negative control.

HEK293T cells treated with nicotine were lysed in 200 μL modified RIPA buffer, a whole cell lysis buffer (Thermo Fisher Scientific, MA, USA). For Western blots we used 40 μg of total protein sample. Protein samples were resolved by 10% SDS-PAGE (Bio-Rad) and transferred to nitrocellulose membranes (Cat: 162-0094, Bio-Rad). Membranes were immune-blotted with rabbit antiserum containing α6 antibody (Lifespan Biosciences, Inc.; LS-C119717), and a primary β-actin antibody (Santa Cruz Biotechnology). Subsequently, HRP-conjugated secondary antibodies were added: anti-rabbit antibody for α6 and anti-mouse antibody for β-actin. β-actin served as the protein loading control. ECL Western Blotting Substrate was used for detection of HRP-antibodies. CL-XPosure film (ThermoFisher Scientific #34090) was developed using an auto-processor in a darkroom.

2.3 Detection of nAChR and taste receptor mRNA using qRT-PCR

Total RNA from HEK293T cells was purified using TRIZOL reagent (cat# 15596029, Thermo Fisher Scientific, MA, USA) and reverse transcription was performed using High-Capacity cDNA Reverse Transcription Kit (cat# 1308188, AB applied biosystems, CA, USA). Total RNA (4 μg) was mixed with 2 μL 10X RT Buffer, 0.8 μL 25X dNTP, 2.0 μL 10X RT Random Primer, 1.0 μL MultiScribe Reverse Transcriptase to total volume of 20 μL per reaction. Reverse transcription was performed at 25ºC x 10 min, then at 37ºC x 120 min, followed by 85ºC for 5 sec and cooled to 4ºC. The products were resolved using 1% agarose gel electrophoresis to determine the expression of nAChR and taste receptor mRNAs. The samples were diluted with 20 μL of RNase-free water to give a total volume of 40 μL. For the detection of nAChR and taste

receptor mRNAs qRT-PCR was carried out by using Applied Biosystems reaction mixture. One μL of 20x TaqMAn Gene Expression Assay, 10 μL of 2x TaqMan Gene Expression Master Mix, 2 μL of cDNA template and 5 μL of RNase-free water was added to a test tube and briefly centrifuged. 20 μL of PCR reaction mix solution was transferred into each well of a 96-well reaction plate and loaded into Applied Biosystems StepOne/StepOnePlus Real-Time PCR system. Reverse transcription were performed at 42°C x 60 min, then 70°C x 5 min and cooled to 4°C. 35 to 40 cycles of PCR amplification were performed (initial denaturation at 95°C for 1 min, denaturation at 95°C for 15 sec, annealing for 15 sec at 53–60°C, and extension for 10 sec at 72°C). RT-PCR products were subjected to electrophoresis on a 1% agarose gel to determine the expression of nAChR subunits and other taste receptors. Human primers were used to detect the presence of mRNAs for the nAChR subunits and are shown in Table 1 and Table 2. The primers were synthesized by Thermo Fisher Scientific.

2.4 Immunoflourescence and Confocal Imaging to localize nAChRs and Taste Receptors in HEK293T cells

HEK293T cells were plated on to a collagen coated 8-well chamber plate and fixed with methanol for 10 min at -20°C. Slides were washed with 200 μL PBS x 3 for 5 min each, then blocking buffer with 3% donkey serum was added to the slide for 1h at room temperature. Subsequently, individual slides were stained with rabbit antiserum containing α3, α4, α5 or β2 antibody (1:100 dilution in 3% donkey serum) or rabbit polyclonal TRPM5 antibody (1:100 dilution in 3% donkey serum). Primary antibodies against α3 (sc-5590), α4 (sc-5591), α5 (sc-376979), β2 (sc-11372), and TRPM5 (sc-27366) were obtained from Santa Cruz Biotechnology, CA, USA.

Slides were washed again with 200 μL PBS x 3 for 5 min each and incubated in the dark

with 1 µL donkey anti-rabbit 488 (1:1000) for 1 h at room temperature. Slides were washed with 200 µL PBS x 3 for 5 min each. Secondary antibody was added to test slides and 3% donkey serum was added to slides used as negative control and stored overnight at 4°C. The slides were incubated with DAPI (1 µg/mL) for 1 min and rinsed with PBS. Coverslip was mounted with a drop of mounting medium. Images were then viewed using a 63x (1.4 numerical aperture) oil immersion objective on a Zeiss LSM 700 confocal laser scanning microscope and processed using ImageJ software with help from Dr. Jie Qian and Ms. Shobha Mummalaneni.

2.5 Calcium Imaging

HEK293T cells were plated onto glass coverslips (Warner Instruments, Hamden, CT, USA) and grown in the incubator at 37°C in 5% CO_2 until they achieved a 75% confluency. Fura-2AM (ab120873; 50 µg) was dissolved in 50 µL of DMSO containing 50 µL of 10% pluronic. Fura-2AM is a membrane-permeant derivative of the Fura-2 dye in which acetoxymethyl ester groups are attached to the dye and are later cleaved by esterases within the cell. Fura-2AM solution was added to 3 mL of normal Ringer's solution and placed on vortex for 10 seconds. Slides mounted on to the bottom of the chamber and washed with 500 µL Ringer's solution x3 containing (in mM) 140 NaCl, 5 KCl, 1 $CaCl_2$, 1 $MgCl_2$, 10 glucose, 10 HEPES, pH 7.4. Fura-2-AM solution (650 µL) was loaded onto each slide and incubated in the dark at room temperature for 2 hours. Slides were washed 3x with Ringer's solution and coverslips were mounted in an experimental chamber (RC-26GLP, Warner Instruments; 0.7 ml volume) and fitted onto a Series 20 Chamber Platform (Warner Instruments). The cells were visualized through a water immersion 40X objective (Zeiss; 0.9 NA) with a Zeiss Axioskope 2 plus upright fluorescence microscope. The image was captured via a cooled CCD camera (Imago, Photonics) attached to an image intensifier (VS4-1845, VideoScope), an epifluorescent light source (Polychrome 5, Photonics), dichroic

filter, and 510 emission filter. The cells were excited with 340 (nm) and 380 (nm) which was visualized at 15 s intervals. Relative changes in Ca^{2+} were expressed as temporal changes in FIR (fluorescence intensity ratio; F_{340}/F_{380}) in individual cells relative to control. The FIR obtained in each cell in control Ringer's solution was normalized to 1. Changes in FIR were analyzed using TILL Vision V3.3 software (TILL Photonics, Martinsried, Germany).

2.6 Detection of Brain-Derived Neurotrophic Factor (BDNF) Synthesis and release in HEK293T cells using ELISA

HEK293T cells were treated with 0.1 μM, 0.25 μM, 0.5 μM, or 1.0 μM nicotine for 30 minutes in the incubator at 37 °C in 5% CO_2. Untreated HEK293T cells were used as negative control.

BDNF was measured in HEK293T cell lysates and culture medium via a sandwich ELISA using the Promega Emax immune assay (Promega Corporation, Madison, WI, USA) according to the manufacturer's protocol. ELISA plates were coated with anti-BDNF mouse antibody (mAb; 1:1000) and incubated overnight at 4°C. Next day the plates were washed and blocked with Blocking Buffer (Promega). BDNF standard or sample (100 μl) was added to each well and incubated with shaking for 2h at room temperature. The plates were washed and anti-human BDNF pAb (1:500; 100 μl) was added to each well and incubated with shaking for 2h at room temperature. After washing, 100 μl of diluted anti-IgY HRP (horseradish peroxidase conjugate; 1:200) was added to each well and developed with TMB (3,3',5,5'-tetramethylbenzidine) solution. The reaction was stopped by adding 100 μl 1N HCl. The absorbance at 450 nm was measured using a VICTOR 2 plate reader and the concentration of BDNF in the samples was calculated from the standard curve and expressed as pg/2x10^6 cells.

Table 1

Primers used for qRT-PCR for Taste Receptors (43)

Gene Product	Sequence	NCBI Reference Sequence
T1R1 F	CGGAGTCTTCTCCTGACTTCA	NM_138697.3
T1R1 R	CCGTGGAGTTGTTTATCTCCTC	
T1R3 F	CCGCCTACTGCAACTACACG	NM_152228.2
T1R3 R	CTAGCACCGTAGCTGACCTG	
T2R38 F	TCCCTGGGAAGGCACATGAG	NM_176817.4
T2R38 R	CAGCACAGTGTCCGGGAATC	
TRPM5 F	GTGACCTGGAGGAGGTGATG	NM_014555.3
TRPM5 R	AGCAGGCTCTTGCGTGAC	

F = forward; R = reverse

https://doi.org/10.1371/journal.pone.0194089.t002

Table 2

Primers used for qRT-PCR to detect the mRNA of nAChRs (43)

Gene Product	Sequence	NCBI Reference Sequence
CHRNA3 F	GGTGGACGACAAGACCAAAG	NM_000743.4
CHRNA3 R	GGGAAGTAGGTCACGTCGATT	
CHRNA4 F	GGAGGGCGTCCAGTACATTG	NM_000744.6
CHRNA4 R	GAAGATGCGGTCGATGACCA	
CHRNA5 F	AAAGATGGGTTCGTCCTGTGG	NM_000745.3
CHRNA5 R	CAAACAAAACGATGTCTGGTGTC	
CHRNA6 F	TGAGACTCTTCGCGTTCCTG	NM_001199279.1
CHRNA6 R	ATTTCAGCTTTGTCATACGTCCA	
CHRNB2 F	CAATGCTGACGGCATGTACGA	NM_000748.2
CHRNB2 R	CACGAACGGAACTTCATGGTG	
CHRNB4 F	AACCCGTTACAATAACCTGATCC	NM_000750.4
CHRNB4 R	ATTCACGCTGATAAGCTGGGC	

F = forward; R = reverse

Except for CHRNA6, all the primers for other CHRNs were same as described by Hochheimer et al. [6]

https://doi.org/10.1371/journal.pone.0194089.t001

Chapter 3: Results

Experiments were designed to investigate nAChRs and Taste Receptor expression in HEK293T cells, and their modulation by nicotine exposure. Parallel studies were performed in cultured adult human fungiform (HBO) taste cells by Dr. Jie Qian to compare nicotine induced changes in nAChRs and taste receptor expression in HBO and HEK 293T cells.

3.1. Expression of mRNAs of nAChR subunits and Taste Receptors in HEK293T cells

As shown in Fig. 5A, using specific primers (Table 1) and RT-PCR, we detected a single band of 132 base pairs (bp) corresponding to T1R3, a single band of 150 bp corresponding to TRPM5, a single band of 346 bp corresponding to T2R38, and a single band of 405 bp corresponding to TRPV1. We also detected a single band of 104 bp corresponding to α3, a single band of 102 bp corresponding to α4, a single band of 233 bp corresponding to α5, a single band of 164 bp corresponding to β2, and a single band of 96 bp corresponding to β4 (Fig. 5B). In addition to the expected band size of 266 bp for α6, we detected a second band of a higher size (Fig. 5B). At present the identification of the second band is not known. These results indicate that HEK293T cells express mRNAs of nAChR subunits and taste receptors.

Figure 5. Gel Electrophoresis after DNA amplification via RT-PCR: Shown below is the detection of **(A)** Taste Receptor and **(B)** nAChR subunit DNA fragments based on size and charge after the amplification of the respective DNA segment via RT-PCR. A single band of expected size was yielded for both each tested subunit with the exception of α6.

5A

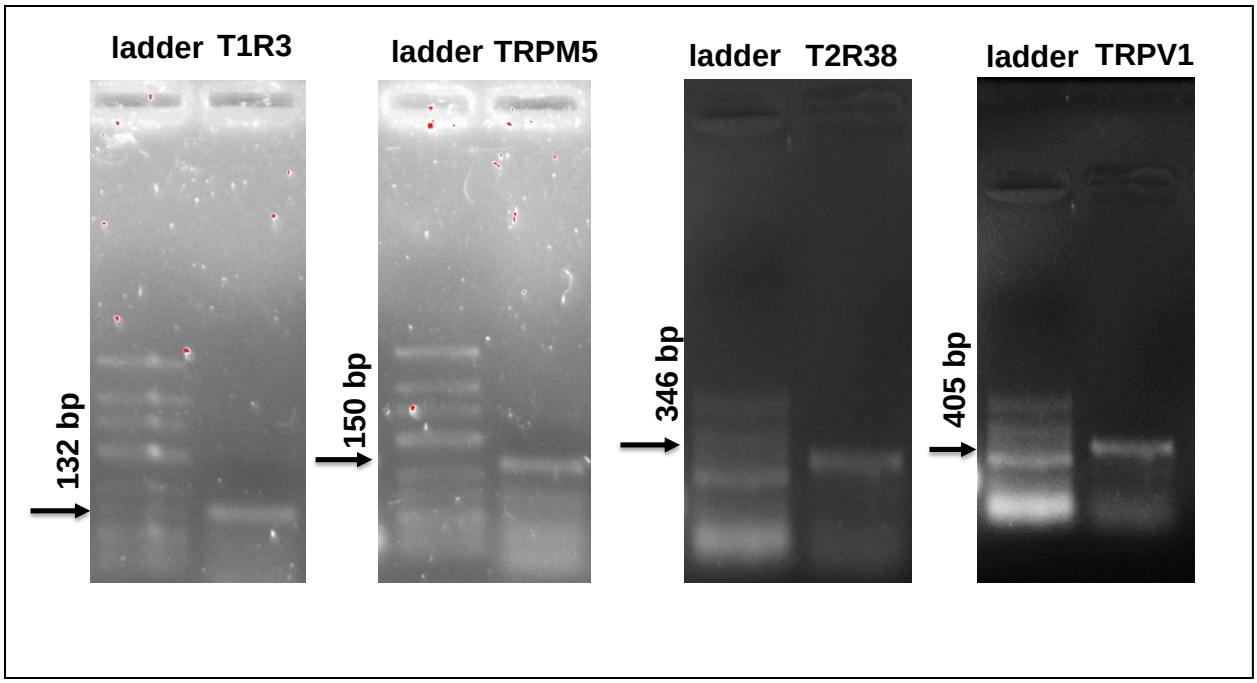
ladder T1R3
ladder TRPM5
ladder T2R38
ladder TRPV1
132 bp
150 bp
346 bp
405 bp

5B

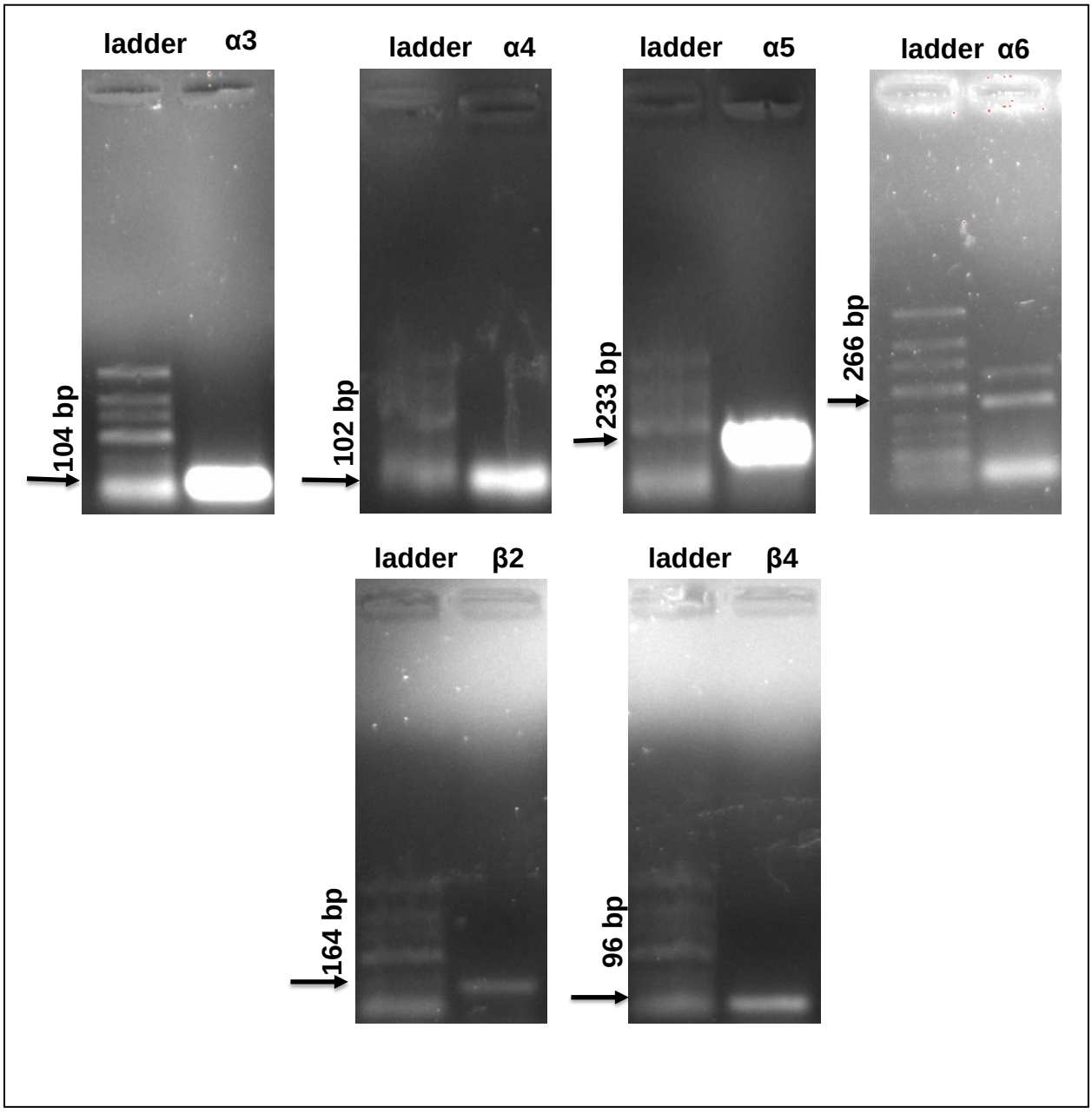
ladder α3
104 bp
ladder α4
102 bp
ladder α5
233 bp
ladder α6
266 bp
ladder β2
164 bp
ladder β4
96 bp

3.2. Expression of nAChR subunit proteins in HEK293T cells

The expression of nAChR proteins was detected by immunofluorescence in HEK293T cells. As shown in Fig. 6, blue-fluorescent DAPI (4',6-diamidino-2-phenylindole) nucleic acid stain was used to identify the nuclei of individual cells. All HEK 293T cells in the visual field were stained with specific nAChR primary antibody labeled with the green fluorescence label. The antibody binding was observed in both the cytosol and the cellular membrane as well as in sub-compartments of cells. Primary antibody was not added to control HEK293T cells and no fluorescence was observed. The specific nAChR subunit location in the apical cell membrane could not be determined (Fig. 6). Dr. Jie Qian characterized the specificity of α4, α6, and β2 antibodies using respective KO mice obtained from Dr. Imad Damaj in the Department of Pharmacology and Toxicology at VCU.

3.3. Co-localization of nAChR subunits in individual HEK293T cells

nAChRs function as pentamers and, while homomeric forms exist, are often found in several heteromeric combinations of α and β subunits. It was hypothesized that HEK293T cells, which we previously demonstrated to contain nAChR subunits, would co-express many subunits in order to form functional ion channels. HEK293T cells were dual-labeled with α5 (green fluorescence) and β2 (red fluorescence) and all cells tested were shown to co-express both nAChR subunits (Fig. 7). Based on results on single nAChR subunit expression, it is believe that all subunits are co-localized within HEK293T cells.

Figure 6. Immunofluorescence of nAChR in HEK293T Cells: Using immunofluorescence, nAChR subunits are visualized in HEK293T cells. DAPI (blue) indicates the cell nucleus.

6

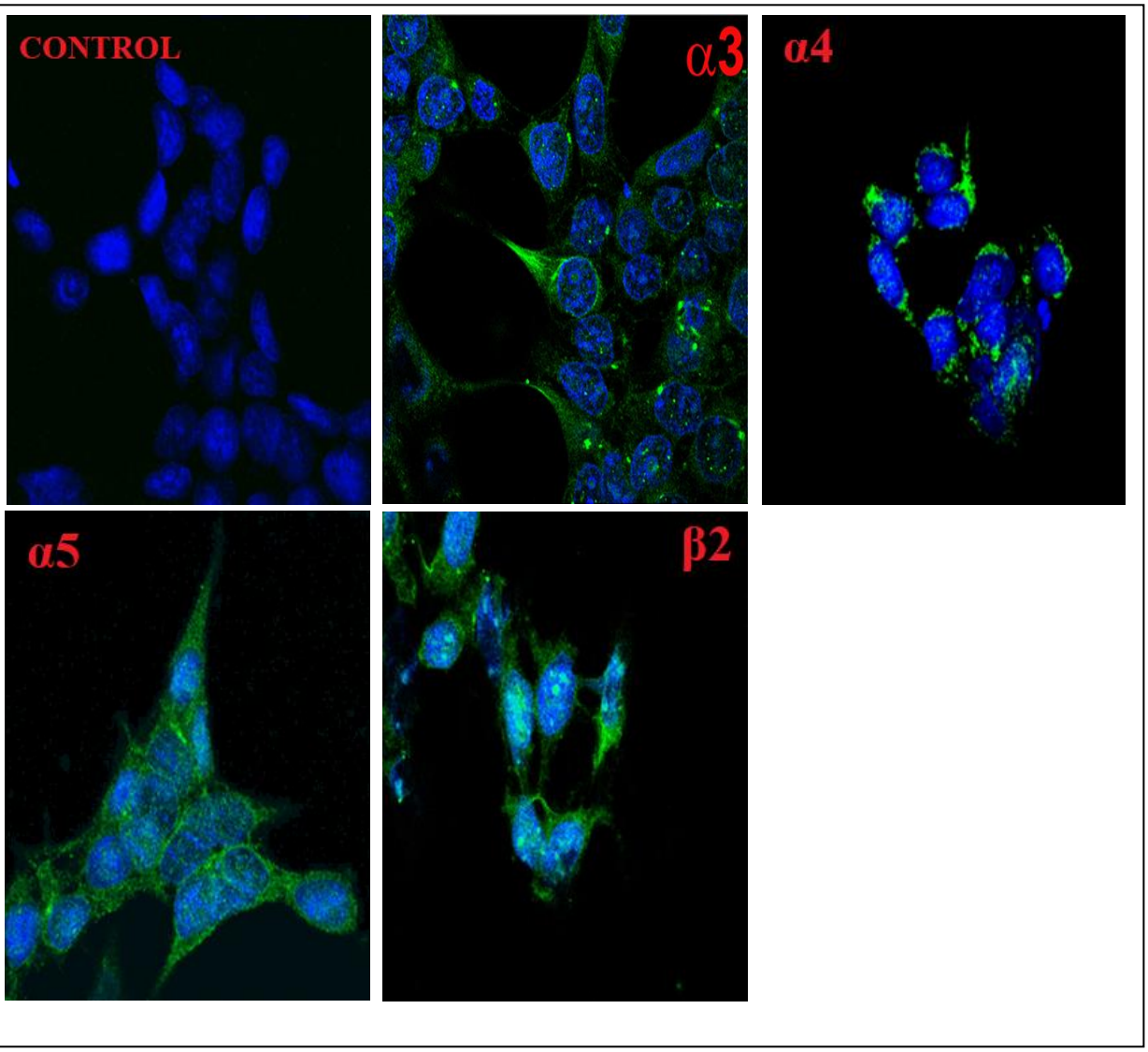

Figure 7. Double-Immunofluorescence nAChR subunits and TRPM5 in HEK293T Cells: Using double-immunofluorescence, the co-localization between nAChR subunits is visualized in an HEK293T cells as well as co-localization between nAChR subunits and TRPM5. DAPI indicates the cell nucleus.

7

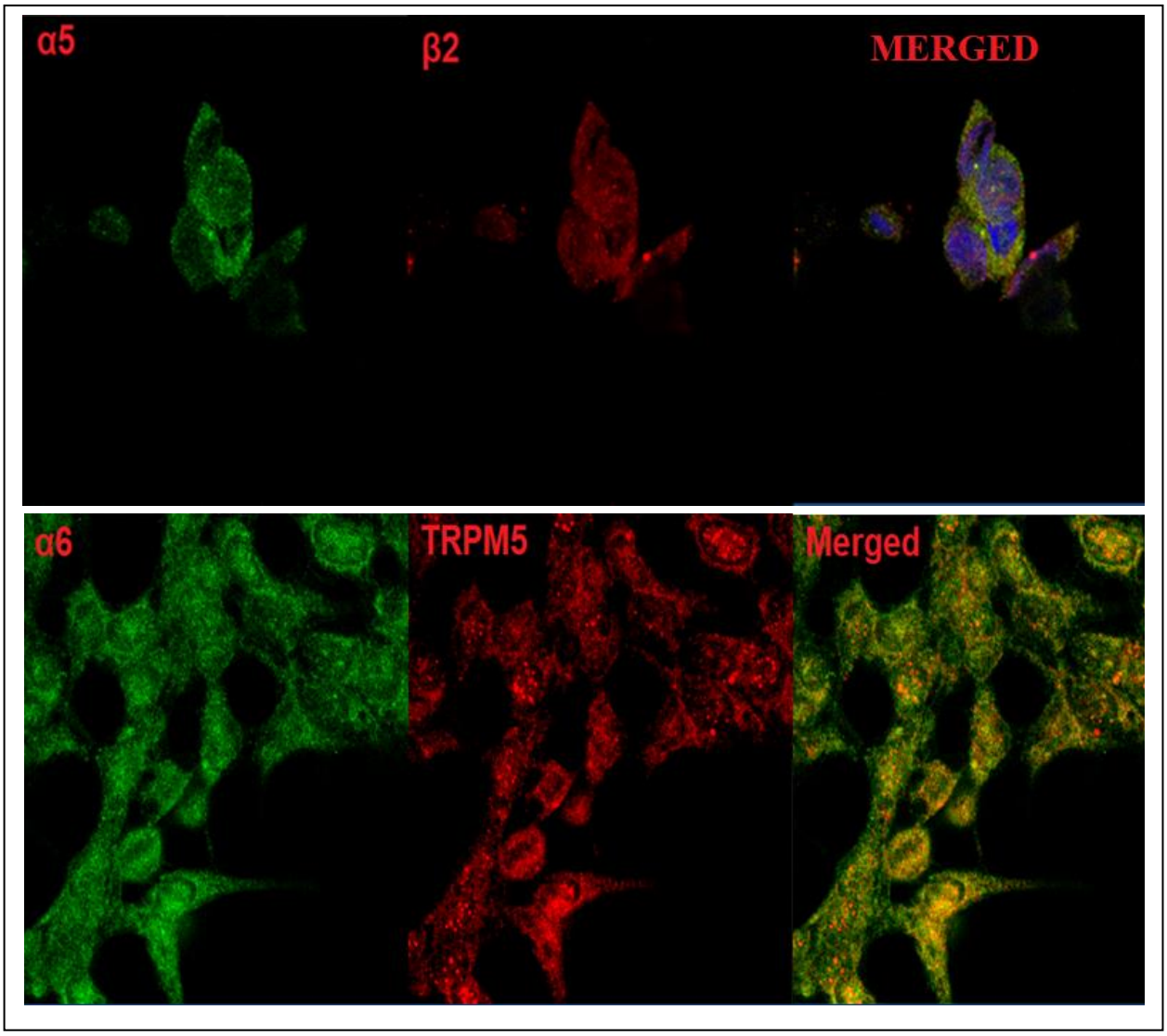

3.4. Co-localization of nAChR subunits and TRPM5 in individual HEK293T cells

Previous results from our lab demonstrated that a subset of HBO cells which expressed nAChR also co-express TRPM5. We hypothesize that the same would occur in HEK293T cells. As also shown in Fig. 7 most of HEK293T cells showed labelling for α6 (green fluorescence) and TRPM5 (red fluorescence) antibodies. This suggests that both TRPM5-dependent and TRPM5-independent (nAChR) receptor mechanisms for nicotine detection are expressed in same cells.

3.5. HEK293T cells express functional nAChR channels

To test if HEK293T cells express functional nAChR channels, we recorded temporal changes in FIR in cells loaded with Fura-2 (Fig. 8) in response to 10 and 100 μM nicotine (Fig. 9). As shown in Fig. 8, Fura-2 loads uniformly in all HEK293 cells. Immediately, following nicotine treatment, the cells responded with a transient increase in $[Ca^{2+}]_i$ (indicated by a rapid increase in FIR). Even in the continuous presence of nicotine changes in $[Ca^{2+}]_i$ returned near their normal value in all cells in the next 60 seconds. The changes in $[Ca^{2+}]_i$ were also found to be dose dependent, increasing in peak FIR value from 1.13 to 1.24 in the presence of 10 and 100 μM nicotine respectively. In summary, the above results indicate that HEK293T cells express functioning nAChRs. The transient changes in $[Ca^{2+}]_i$ reflect that HEK293T cells are healthy and regulate $[Ca^{2+}]_i$ to maintain cell homeostasis even in the presence of nicotine.

Figure 8. HEK293T cells loaded with Fura-2 at 340 (nm) and 380 (nm): The images represent HEK293T cells loaded with Fura-2 uniformly distributed in the cytosol and retained inside the cell.

8

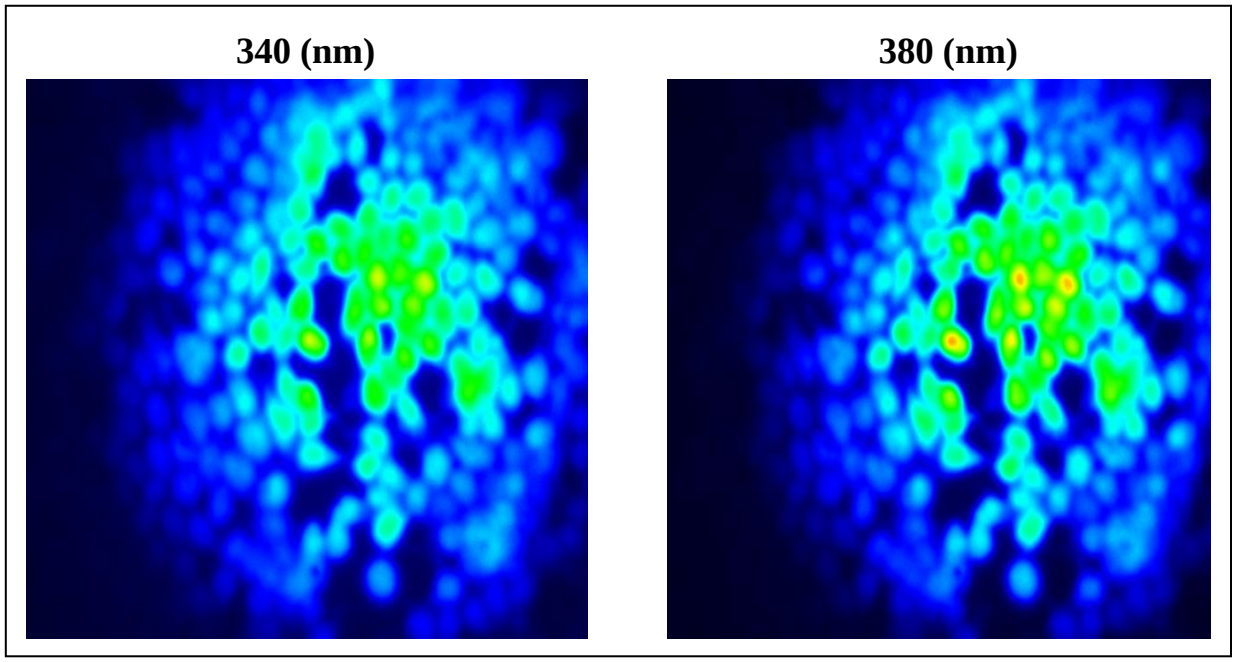

Figure 9. Ca^{2+} measurement in HEK293T Cells: This graph shows changes of $[Ca^{2+}]_i$ upon presentation of 10 and 100 μM nicotine in Ringer's solution. The FIR values in control Ringer's solution were normalized to 1. Data is presented as the mean ± SEM; n=92.

9

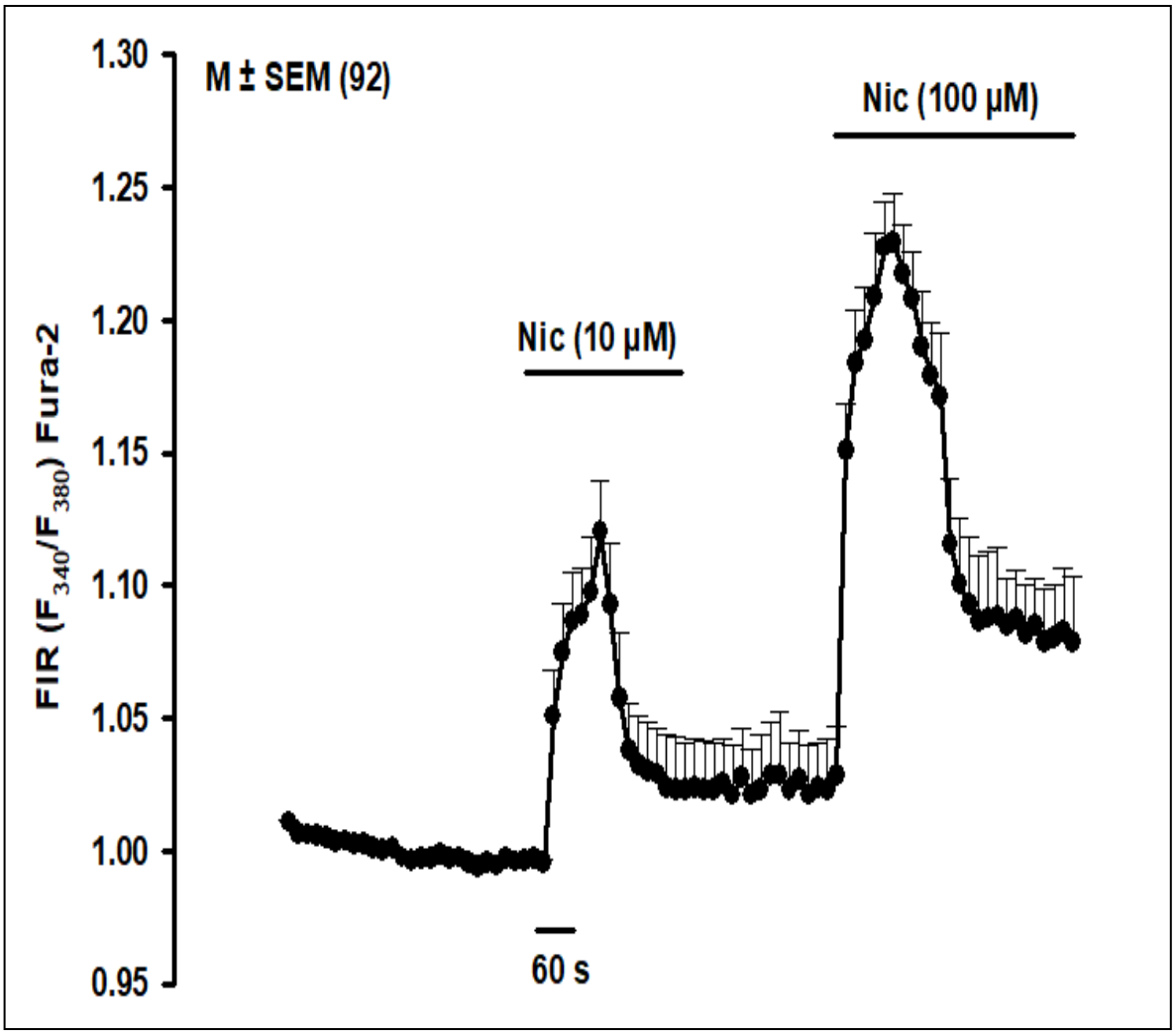
M ± SEM (92)
Nic (100 µM)
Nic (10 µM)
FIR (F340/F380) Fura-2
1.30
1.25
1.20
1.15
1.10
1.05
1.00
0.95
60 s

A follow-up experiment was conducted in the presence of TPPO, a TRPM5 blocker, to determine if nicotine effects on $[Ca^{2+}]_i$ are independent of TRPM5. In the presence of a mixture containing 10 μM nicotine and 50 μM TPPO, $[Ca^{2+}]_i$ showed a transient increase which was less than in the presence of 10 μM nicotine alone (Fig. 10). Peak FIR value was shown to decrease from 1.22 to 1.16, an overall decrease of 20.59%. These results indicate that a major component of the effect of nicotine in HEK293T cells is TRPM5-independent.

3.6. Nicotine-induced changes in nAChR subunit and Taste Receptor mRNAs in HEK293T cells

To determine the effects of nicotine on nAChR mRNA expression, cultured HEK293T cells were incubated with nicotine at 0.25, 0.5, and 1.0 μM for 24 hours. Changes in nAChR mRNAs were measured using qRT-PCR. nAChR α5 increased significantly at 0.25 ($p = 0.002$) and 0.5 μM nicotine ($p = 0.001$). However, relative to 0.5 μM nicotine, no further increase in its expression was observed at 1 μM nicotine (Fig. 11A). nAChR α6 increased significantly at 0.25 ($p < 0.001$), 0.5 ($p < 0.001$) and 1.0 μM nicotine ($p = 0.003$). However, relative to 0.5 μM nicotine, no further increase in its expression was observed at 1 μM nicotine (Fig. 11B). nAChR β2 increased significantly at 0.5 ($p = 0.025$) and 1.0 μM nicotine ($p = 0.002$). However, relative to 0.5 μM nicotine, no further increase in its expression was observed at 1 μM nicotine. These results suggest that nicotine produces maximum increase in α5, α6, and β2 nAChR mRNAs at 0.5-1 μM nicotine (Figure 11C).

Next, we also tested the effect of nicotine on the mRNA of human bitter taste receptor T2R38 under the same conditions. T2R38 increased significantly at 0.25 ($p = 0.001$), 0.5 ($P < 0.001$) and 1.0 μM nicotine ($p < 0.001$). In this case the increase in T2R38 mRNA at 1 μM

Figure 10. Ca^{2+} measurement in HEK293T Cells in the presence of TRPM5 Blocker: This graph shows changes of $[Ca^{2+}]_i$ upon presentation of 10 μM nicotine and 50 μM TPPO, a TRPM5 blocker, in Ringer's solution. The FIR values in control Ringer's solution were normalized to 1. Data is presented as the mean ± SEM; n=12.

10

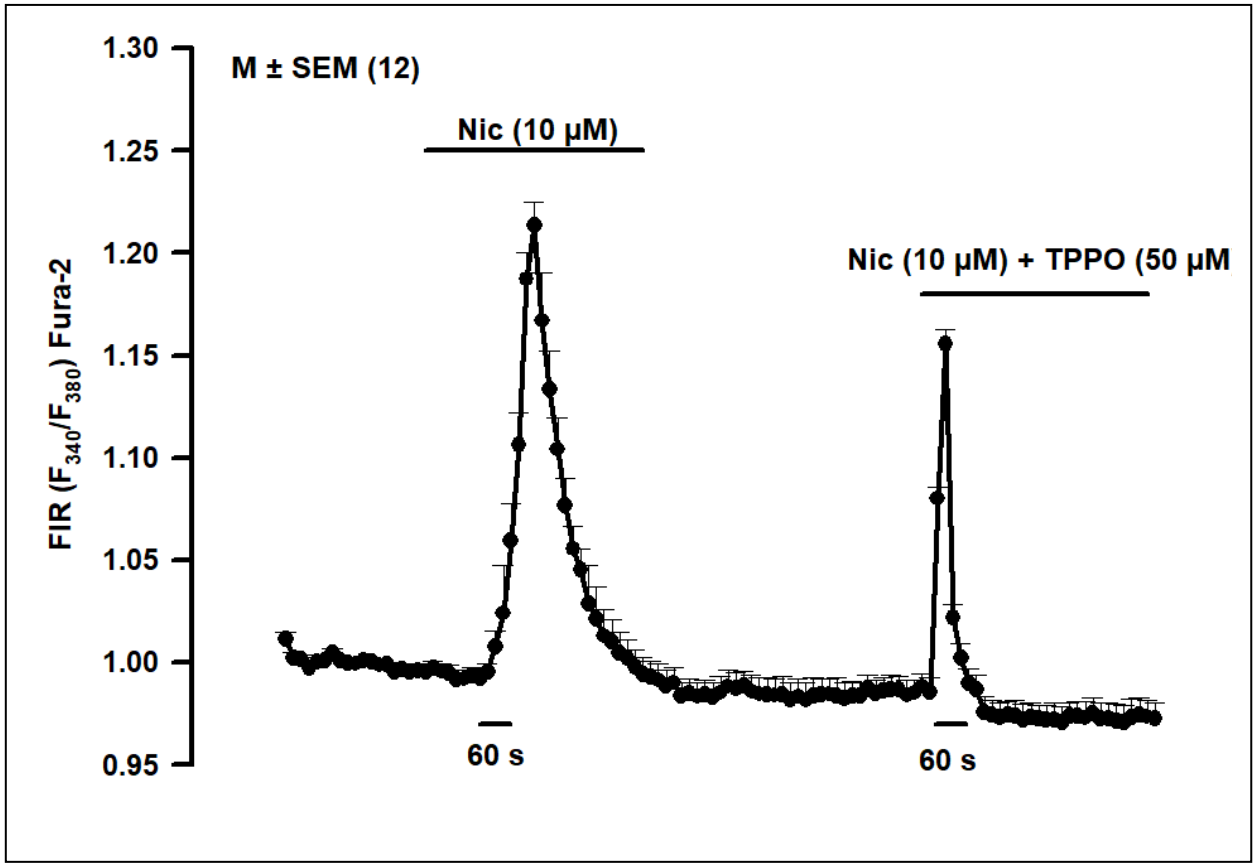
M ± SEM (12)
Nic (10 μM)
Nic (10 μM) + TPPO (50 μM
FIR (F340/F380) Fura-2
1.30
1.25
1.20
1.15
1.10
1.05
1.00
0.95
60 s
60 s

nicotine was less than at 0.5 μM nicotine (p=0.00029). Thus nicotine produced a maximum increase in T2R38 mRNA expression at 0.5 μM nicotine in a biphasic manner (Figure 12). These results suggest that both nAChR and taste receptors change dynamically with nicotine exposure. We hypothesize that changes in their expression with nicotine exposure may reflect adaptation to the taste of chronic bitter taste of nicotine under chronic exposure.

3.7. Effect of nicotine on nAChR protein expression in HEK293T cells

A western blot was performed to determine if there was a correlation between increased mRNA expression (Figure 13) and an increase in protein expression. nAChR α6 was tested as the differential change in mRNA between HEK293T and HBO cells were observed in this subunit. HEK293T cells were incubated with 0.25, 0.5, and 1.0 μM nicotine for 24 hours. nAChR α6 increased significantly at 0.25 ($p = 0.0196$), 0.5 ($p = 0.0172$), and 1.0 μM nicotine ($p = 0292$) with a maximum increase at 0.5 μM.

3.8. Effect of nicotine on BDNF concentration and release in HEK293T cells

ELISA was conducted to determine the effect of nicotine on synthesis and release of BDNF, a neuropeptide involved in maturation of taste buds and nerve formation synaptic connections between the taste buds and cranial nerves, typically activated through acetylcholine. Treating HEK293T cells with 0.25 μM nicotine significantly increased the content in cell lysate that remained elevated at 0.5 and 1.0 μM nicotine. Relative to control, treating HEK293T cells with 0.25, 0.5 and 1.0 μM nicotine produced a small but dose dependent increase in BDNF concentration in the both the cell lysis and media (Figure 14). However, nicotine was shown to be a poor signal for the release of BDNF as the majority of BDNF remained within the cell.

Figure 11. qRT-PCR for nAChR subunit mRNA expression: The values are presented as the mean ± SEM mRNA nAChR subunit expression between negative control and 24 hour nicotine exposure at variable concentrations. The asterisk represents a significant difference (ANOVA < 0.05) between control and treatment conditions. Figure data was normalized to GAPDH. **(A)** α5 mRNA expression was shown to significantly increase at 0.25 μM and 0.5 μM nicotine (ANOVA=0.002 and 0.001 respectively). **(B)** α6 mRNA expression was shown to significantly increase at 0.25 μM, 0.5 μM, and 1.0 μM nicotine (ANOVA<0.001, <0.001, and 0.003 respectively). **(C)** β2 mRNA expression was shown to significantly increase at 0.5 μM and 1.0 μM nicotine (ANOVA=0.025 and 0.003 respectively).

11A

	WT	0.25 µM Nic	0.5 µM Nic	1.0 µM Nic
Fold Change	1	1.21	1.58	1.3
ANOVA	1	0.00176	0.0007	0.09074

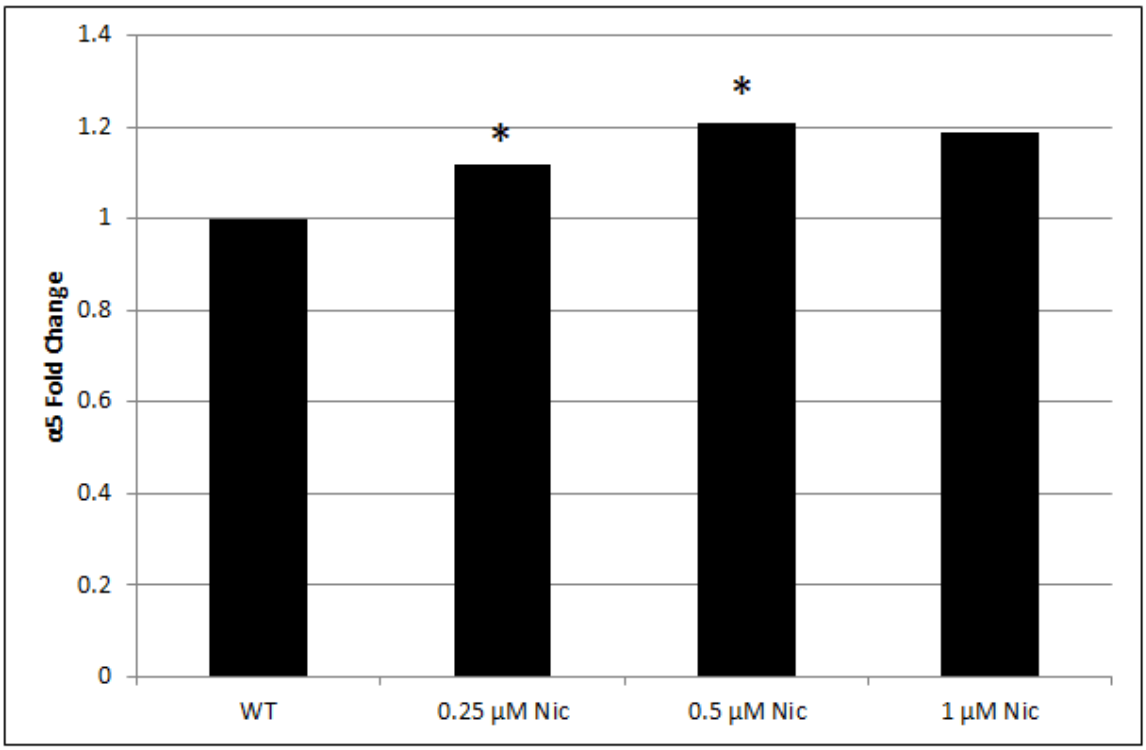

11B

	WT	0.25 µM Nic	0.5 µM Nic	1 µM Nic
Fold Change	1	1.42	1.59	1.4
ANOVA	1	0.00003	0.00017	0.00305

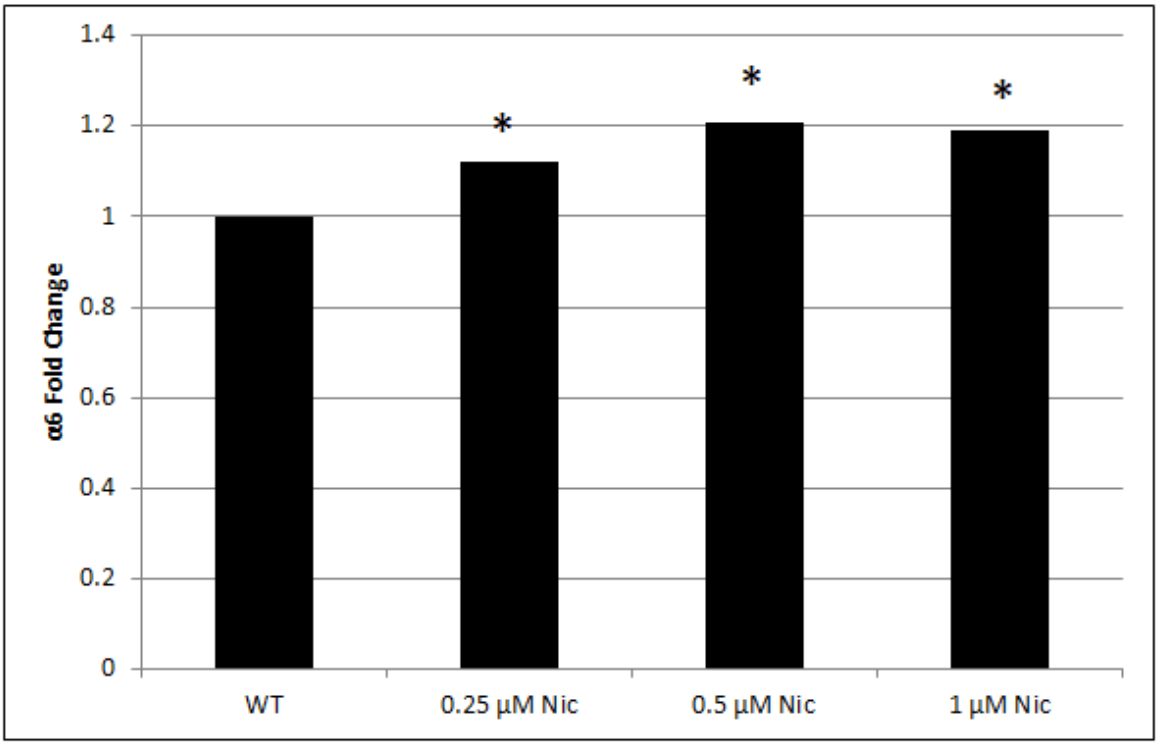

11C

	WT	0.25 µM Nic	0.5 µM Nic	1 µM Nic
Fold Change	1	1.12	1.21	1.19
ANOVA	1	0.05767	0.02485	0.00258

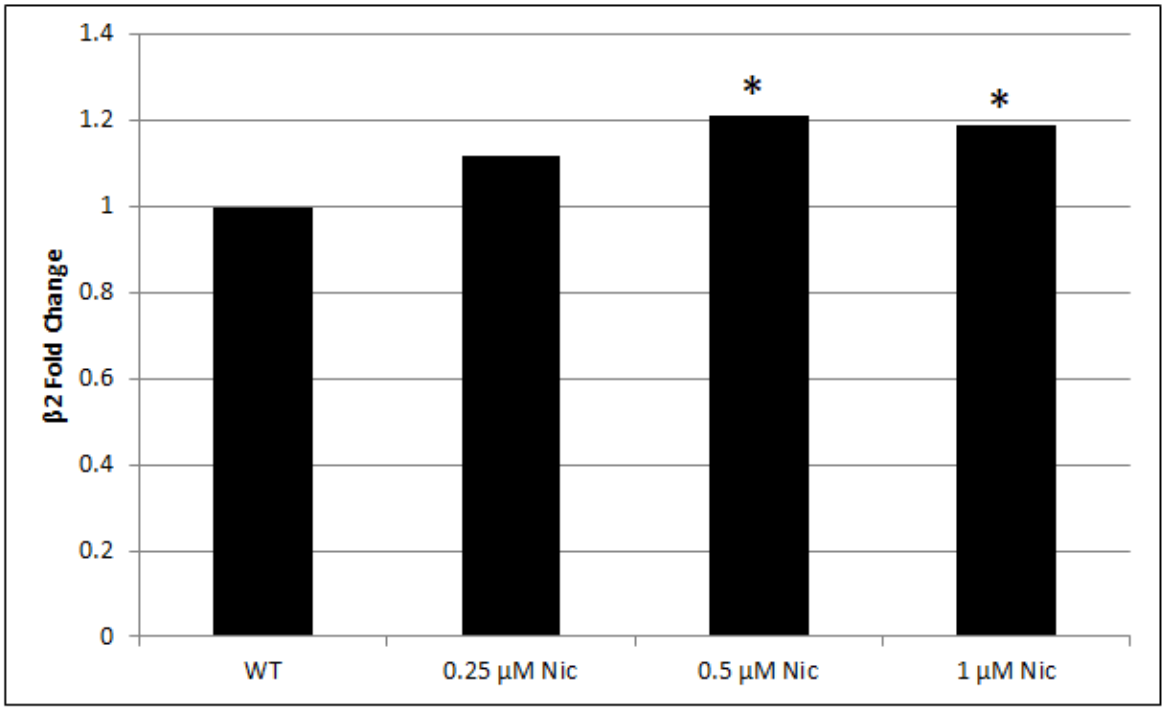

Figure 12. qRT-PCR for T2R38 mRNA expression: The values are presented as the mean ± SEM mRNA T2R38 mRNA expression between negative control and 24 hour nicotine exposure at variable concentrations. The asterisk represents a significant difference (ANOVA < 0.05) between control and treatment conditions. Figure data was normalized to GAPDH. T2R38 mRNA expression was shown to significantly increase at 0.25 μM, 0.5 μM, and 1.0 μM nicotine (ANOVA =0.001, < 0.001, and <0.001 respectively).

12

	WT	0.25 µM Nic	0.5 µM Nic	1 µM Nic
Fold Change	1	1.26	1.69	1.47
ANOVA	1	0.00102	2.7E-05	0.00029

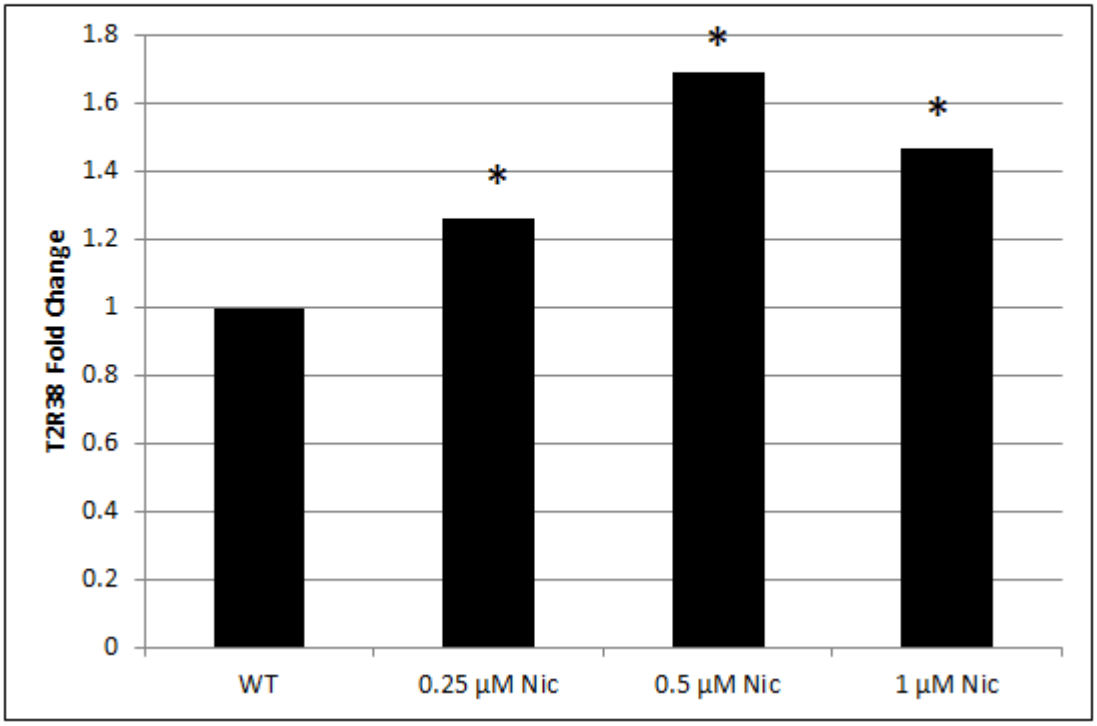

Figure 13. The effect of Nicotine on nAChR subunit protein expression in HEK293T Cells: **(A)** Protein expression captured through ImageJ software of Western Blot results. **(B)**This data shows HEK293T cells which were treated with varying amounts of nicotine for 24 hours and the expression level of nAChR α6 subunit protein was measured using Western Blot analysis. The asterisk represents a significant increase [p = 0.020, 0.017, and 0.029 respectively] in expression at 0.25 μM, 0.5 μM, and 1.0 μM nicotine. The values of protein expressions are normalized to β-Actin.

13A

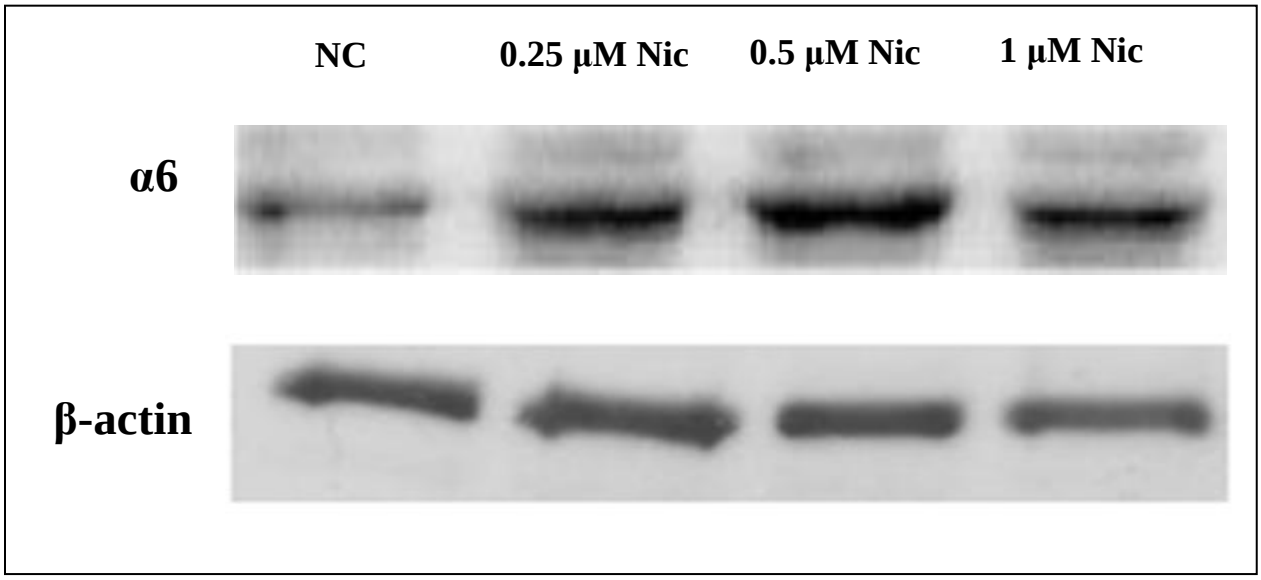

13B

	NT	0.25 µM Nic	0.5 µM Nic	1 µM Nic
fold change	1	6.36	8.66	6.82
P-Value	1	0.01953	0.01721	0.02925

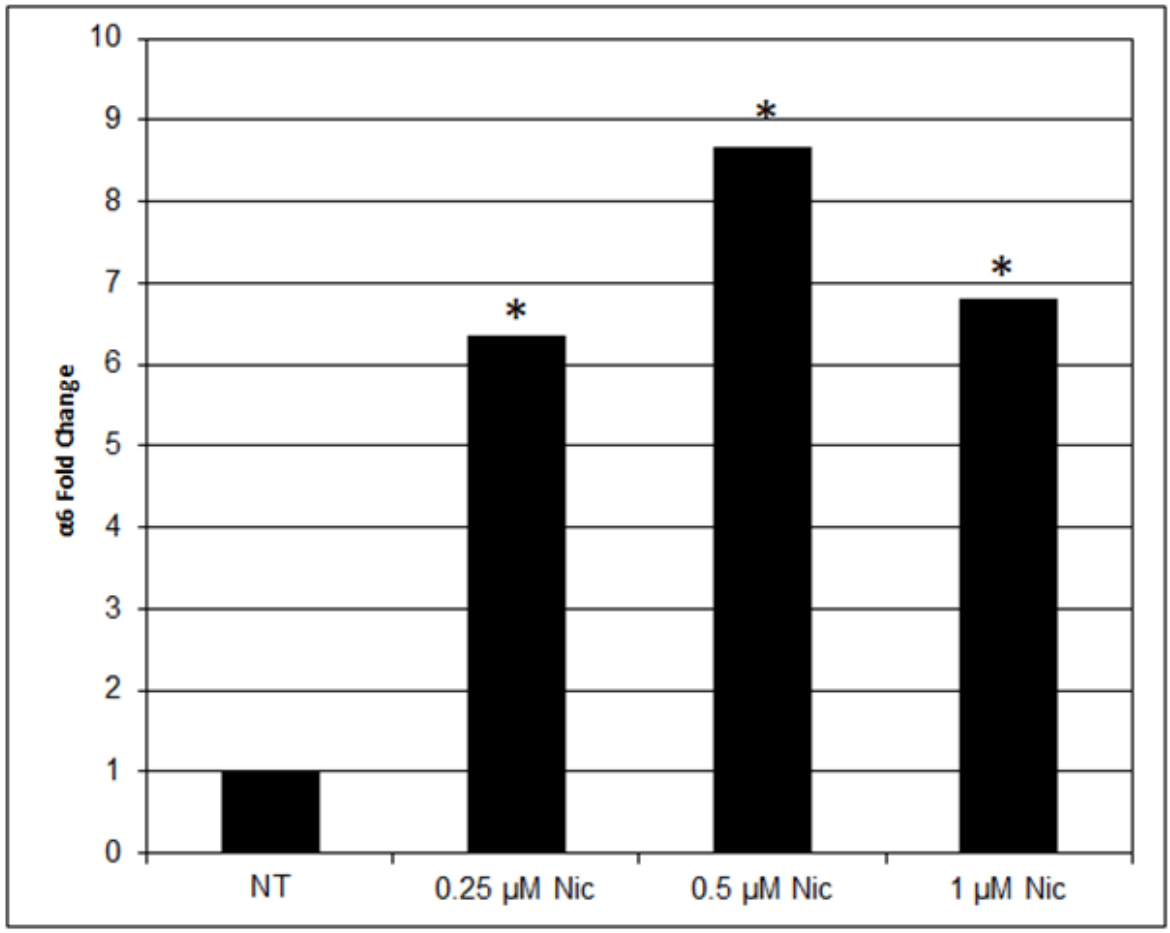

Fig 14. Effect of Nic on BDNF synthesis and release in HEK293T cells: This graph shows changes to BDNF synthesis and release based on nicotine exposure in HEK293T cells. Relative to control, at 0.25 μM Nic, BDNF concentration in cell lysate was significantly increased ($p = 0.0001$), and remained elevated at 0.5 μM ($p = 0.0331$) and 1.0 μM Nic ($p = 0.0041$). Relative to control at 0.25 μM, 0.5 μM, and 1.0 μM Nic, a small but significant increase in the BDNF concentration was observed in the media ($p = 0.0001$). The values are mean ± SEM of triplicate measurements.

14

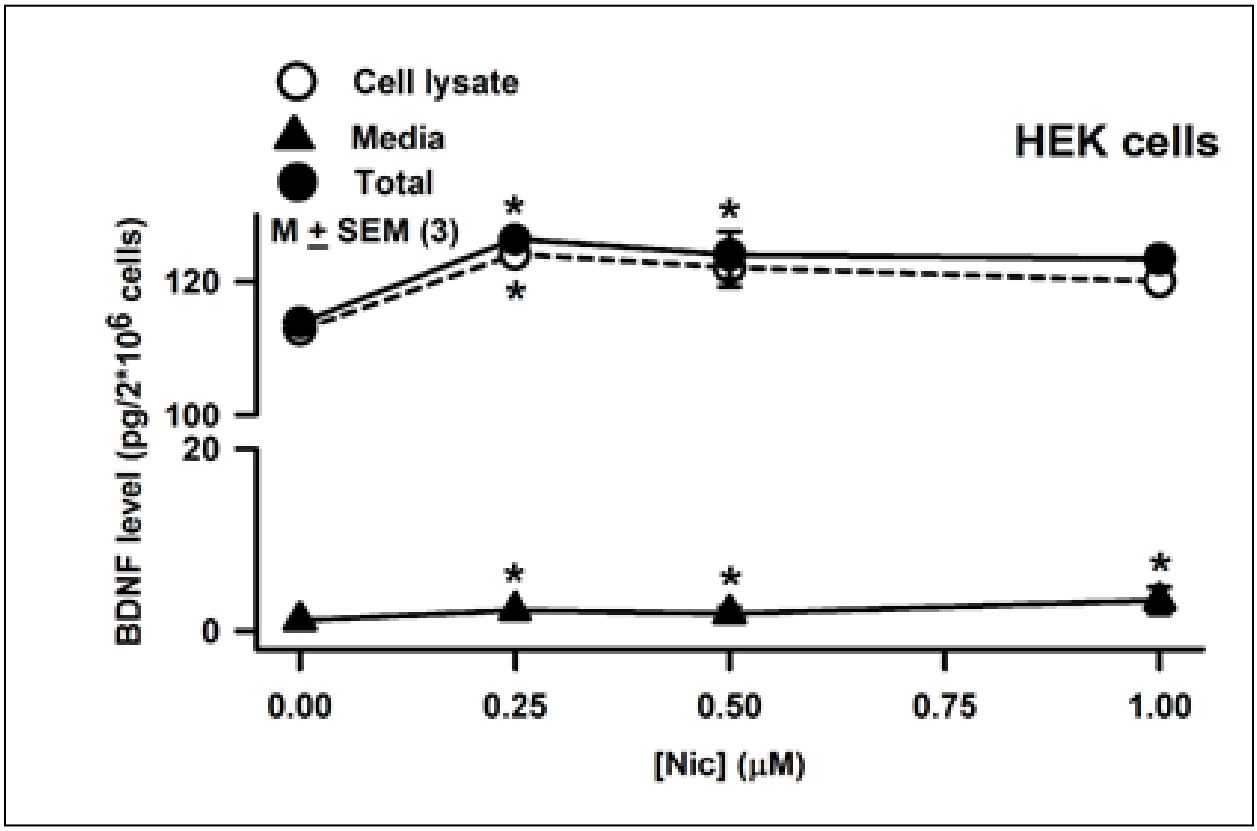
Cell lysate
Media
Total
HEK cells
M ± SEM (3)
BDNF level (pg/2*10^6 cells)
120
100
20
0
0.00
0.25
0.50
0.75
1.00
[Nic] (μM)

Chapter 4: Discussion

The nAChRs have been shown to be expressed in rat taste cells, mouse small intestine (STC-1) cells in culture, enteroendocrine cells of the mouse gut, HBO cells, and in this study we present new results that demonstrate their expression in HEK293T cells (58, 59, 76). In relation to taste transduction, nAChR-positive TRCs co-expressed in T2R38 (59). While only a specific subset of cells were found to express nAChRs in HBO and mouse enteroendocrine gut cells, the entire population of STC-1 and HEK293T cells expressed nAChRs (58, 59, 76). Furthermore, all nAChR-positive cells co-expressed TRPM5. Sweet, bitter, umami, salty and sour taste receptors are expressed in distinct non-overlapping taste receptor cells. This is a unique property of differentiated TRCs versus undifferentiated HEK293T cells. The nAChRs are expressed in TRPM5-positive and T2R38-positive HBO cells. Thus, nAChRs also serving as bitter taste receptors for nicotine are expressed in cells which detect bitter taste via T2Rs. Thus, both TRPM5-dependent and TRPM5-independent pathways are present in same T2R-TRPM5-positive TRCs.

In a patch clamp study conducted on isolated rat taste receptor cells, 2 out of 10 (20%) taste cells responded with an increase in inward current when exposed to nicotine (58). Nicotine (0.2 mM) elicited inward currents that were inhibited in the presence of 0.3 mM Mecamylamine (58). The nicotine-induced current reversed near -10 mV, as expected for poorly selective nAChR channels (58). Thus, nicotine elicits currents in a subset of fungiform TRCs by activating nAChRs (58). These currents are most likely related to the CT responses to nicotine and their sensitivity to mecamylamine. A similar fraction of TRCs was found to express nAChR proteins in immunofluorescence studies. Only 2 of 11 HBO cells (18%) investigated were observed to express the α5 subunit. This further strengthens the hypothesis that differentiated taste bud cells express

specific taste receptors in non-overlapping subsets of TRCs (43). As undifferentiated cells, the entire population of the HEK293T cells demonstrated the expression of nAChRs.

In rodents, CT responses to nicotine were inhibited by topical lingual application of 8-chlorophenylthio (CPT)-cAMP, a membrane permeable cAMP analog, and loading taste cells with $[Ca^{2+}]_i$ by topical lingual application of ionomycin and $CaCl_2$ (58). In contrast, CT responses to nicotine were enhanced when TRC $[Ca^{2+}]_i$ was reduced by topical lingual application of BAPTA-AM (58). This indicates that a different transduction mechanism is used to transduce TRPM5-independent but nAChR-dependent receptor mechanism that is regulated by cAMP and $[Ca^{2+}]_i$. However, further experiments are needed to determine if nAChR-dependent mechanism also leads to ATP release following nicotine stimulation. Since nicotine elicits CT nerve responses in TRPM5-KO mice, it is likely that, if not ATP, another neurotransmitter may be involved. In addition, correct identification of nicotine remains above chance in rats given both nicotine and mecamylamine, suggesting the importance of this TRPM5-dependent pathway in transduction of nicotine as TRPM5 is not blocked by mecamylamine (40).

We have demonstrated that HEK293T cells express the necessary mRNAs involved in both TRPM5-dependent (Fig. 5A) as well as TRPM5-independent pathway (Fig. 5B), similar to previous results found in HBO cells (S1 Fig.) (43). However a key distinction is made through immunofluorescence when comparing the populations of HBO and HEK293T cells which endogenously express both receptor types. HEK293T cells express each nAChR subunit as well as TRPM5, a downstream signaling component of umami, sweet, and bitter taste reception throughout the population (Figs. 6 and 7), while HBO cells express these proteins uniquely in specific subsets of non-overlapping cells (S2 Fig.) (43). While the entirety of the population of HEK293T cells was found to express α5, HBO cell results demonstrated only 2 of 11 cells (18%)

expressed the α5 subunit (43). The subset of nAChRs-positive HBO cells was found to co-express TRPM5 specifically while nAChR-negative cells did not, unlike the complete expression seen throughout the HEK293T population (43). In addition, a subset of HBO cells responded to an increase in $[Ca^{2+}]_i$ when exposed to nicotine in a dose-dependent manner (S4 Fig.) whereas the entire population of HEK293T cell demonstrated an increase in $[Ca^{2+}]_i$ with nicotine (Fig. 9).

Comparison of CT responses to nicotine between WT and TRPM5 KO mice, the KO mice showed a diminished but residual response relative to WT mice (58). A similar decrease in CT response was noted when comparing control WT mice to WT mice in which the tongue was stimulated with a solution containing nicotine + mecamylamine, a non-selective nAChR blocker (58). In HBO cells at nicotine concentrations less than 5 mM, nAChRs and T2Rs each account for about 50% of the total response to nicotine (58). Above 5 mM nicotine, the T2R fraction reached its maximum response and the nAChRs begins to predominate (58). Consequently at 10 mM nicotine the T2R response fraction decreases to 41% and at 20 mM nicotine it is 35% and 30% in the high concentration limit (58). Since the TRPM5-dependent response (T2R component) is mecamylamine-insensitive, in the presence of mecamylamine, the T2R component in the high concentration limit represents a higher fraction of the CT response, i.e. 41% (58). Thus the two pathways, TRPM5-independent and TRPM5-dependent, detect nicotine at different concentration ranges. These results were mirrored in our own HEK293T studies in calcium imaging, where the addition of TPPO (50 μM), a TRPM5 blocker, reduced peak response to nicotine by 21% in low concentrations of nicotine (10 μM). A higher concentration of nicotine was used in recording CT responses by directly stimulating the rodent tongues and require higher concentrations of nicotine to elicit a CT response. It is hypothesized that both blockers would have a similar impact on each of the cell types. HEK293T cells are commonly used to overexpress nAChRs to study channel

function and regulation. The presence of both a TRPM5-independent and TRPM5-dependent pathways for nicotine facilitates an extended range of concentrations through which nicotine can bind to relevant receptors.

In the kidney, α7 nAChRs are expressed in the proximal and distal tubules and exposure to nicotine in these cells has been demonstrated to be involved in the progression of chronic kidney disease (CKD) (73, 74). Identification of nAChRs within HEK293T, an embryonic kidney cell line, could suggest a link between over express of nAChRs and kidney disease.

In addition, Ca^{2+} influx along with cell depolarization mediated by some types of nAChRs can produce neurotransmitter and hormone release. The taste system is inherently plastic due to the turnover of receptor cells every 10 to 14 days in humans (79). Under the influence of varying environmental factors, different proportions of receptor membrane components can be incorporated as new taste receptor cells dependent upon the hormonal, dietary, and developmental status of the animal (79). As taste receptor cells are replaced approximately every 10 to 14 days in humans, the effect of nicotine exposure on synthesis and release of BDNF raises a concern. In enteroendocrine cells, BDNF plays a key role in survival and growth of enteric neurons, augmentation of enteric circuits, and stimulation of intestinal peristalsis and propulsion (76). In taste, BDNF is responsible for the formation and maturation of TBCs and innervating nerve fibers (43). BDNF-KO mice were demonstrated to lack the sense of taste and taste transduction (80). Our results demonstrated that, while in both HBO and HEK293T exposure to the nicotine increased BDNF synthesis, only HBO cells released significant amount of BDNF in response to nicotine. In HEK293T cells, a lack of nicotine induced BDNF release may signify a decreased ability of undifferentiated cells to release hormones and neurotransmitters.

In vitro experiments conducted in this study mimic physiologically relevant concentrations of nicotine in both short and long-term exposure to HEK293T ad HBO cells. Short-term exposure to nicotine concentrations can reach mM amounts based on the source through which nicotine is ingested orally, in particular while chewing tobacco (5). In HBO cells, these concentrations were demonstrated to elicit significant $[Ca^{2+}]_i$ flux responses (43). In CT recordings in rodents mM nicotine concentrations elicited dose-dependent increase in the CT response. Long-term exposure to nicotine typically increases nicotine concentrations in human saliva in the range of 0.1 to 0.2 μM. When HEK293T and HBO cells were exposed to nicotine at sub-micromolar concentrations *in vitro,* nicotine induced up-regulation of nAChR mRNA and protein expression (43). Exposure of nicotine in HEK293T also demonstrated up-regulation of T2R38 expression. An important distinction arises when comparing the fold-change in mRNA and protein expression between HBO and HEK293T cells. Nicotine up-regulated α6 mRNA expression to approximate 1.6 and 20-fold in in HEK293T and HBO cells, respectively (43) (S5 Fig.). These changes in nAChR expression would likely increase the sensitivity to nicotine within the taste system via the TRPM5-independent but nAChR-dependent pathway. In addition to changes in nAChRs, nicotine also increased T2R38 expression in HEK293T cells in a biphasic manner, with a relative maximum at 0.5 μM nicotine, same as with the nAChR subunits. T2R38 was not tested on HBO cells, but it is hypothesized to increase in a similar manner seen in HEK293T cells. At present it is not clear if the expression of other T2Rs is increased by acute or chronic exposure to nicotine in HEK293T or HBO cells.

Our study indicates that many nAChR subunits are expressed in HEK293T cells endogenously. These native nAChRs may influence the characteristics of over-expressed nAChR channels and the expression of these nAChRs can be readily influenced through short-term

nicotine exposure as shown in our qRT-PCR studies. Up-regulation of these nAChR subunits in HEK293T and HBO cells was shown to occur with nicotine exposure as low as 0.25 μM nicotine, mimicking serum and saliva nicotine concentrations in smokers (5, 43). Up-regulation of nAChRs has also been observed in human dermal fibroblasts as well and in human squamous lung cancer cell lines (77, 78).

Further investigations into nAChRs and their role in parallel with TRPM5-dependent pathways should focus on determining if nicotine effects on BDNF release are blocked by nAChR blocker, mecamylamine. Another focus be to resolve if bitter taste of ethanol is also transduced via nAChRs and additive effects of nicotine and ethanol on the taste system occur via nAChRs expressed in TRCs. Next, nicotine induced release of ATP could be measured in HBO cells to understand if both TRPM5-dependent and TRPM5-independent pathways ~~the~~ use ~~of~~ this taste-specific neurotransmitter elicit neural responses to nicotine stimulation. A final focus should consider long-term effects of nicotine exposure on expression of relevant receptors as well as their recovery upon nicotine abstinence.

SUPPLEMENTAL FIGURES

1

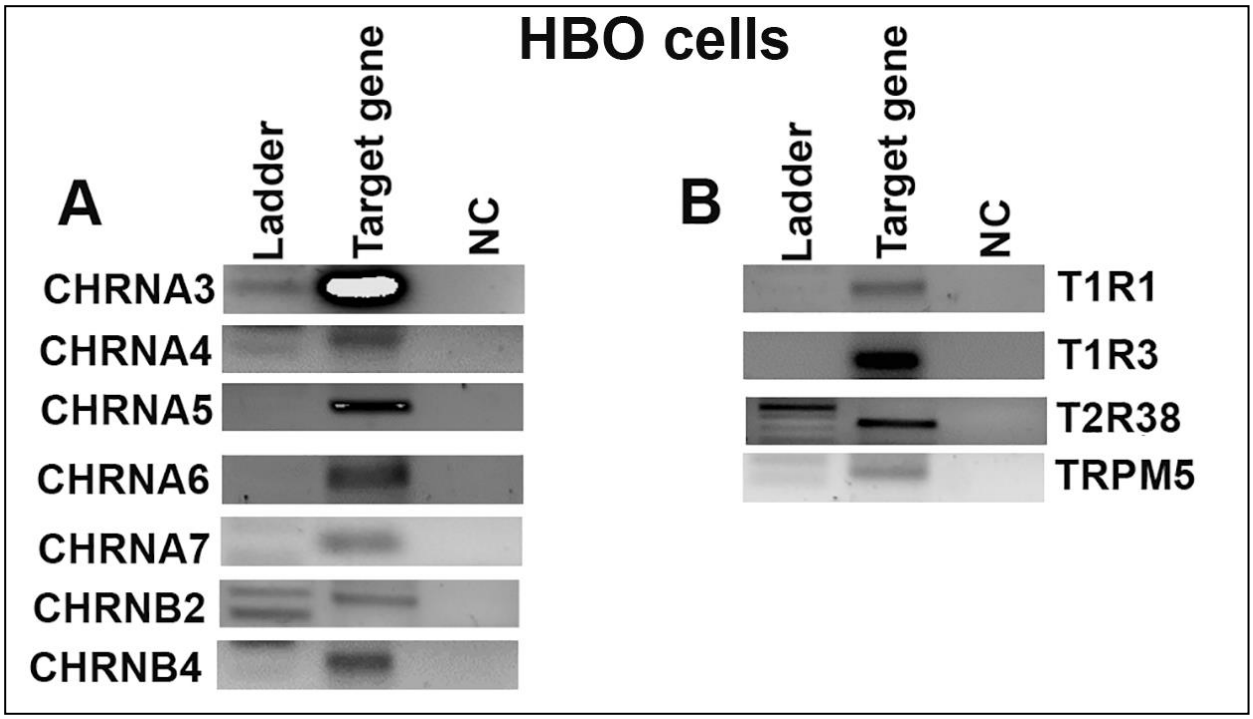

Supplemental Figure 1. Expression of nAChR subunits, taste receptors, and intracellular signaling intermediates in HBO (43):
(A) mRNAs for the α3, α4, α5, α6, α7, β2, and β4 were detected in HBO cells. **(B)** In addition, mRNAs for T1R1, T1R3, T2R38, and TRPM5 were detected in HBO cells.

2

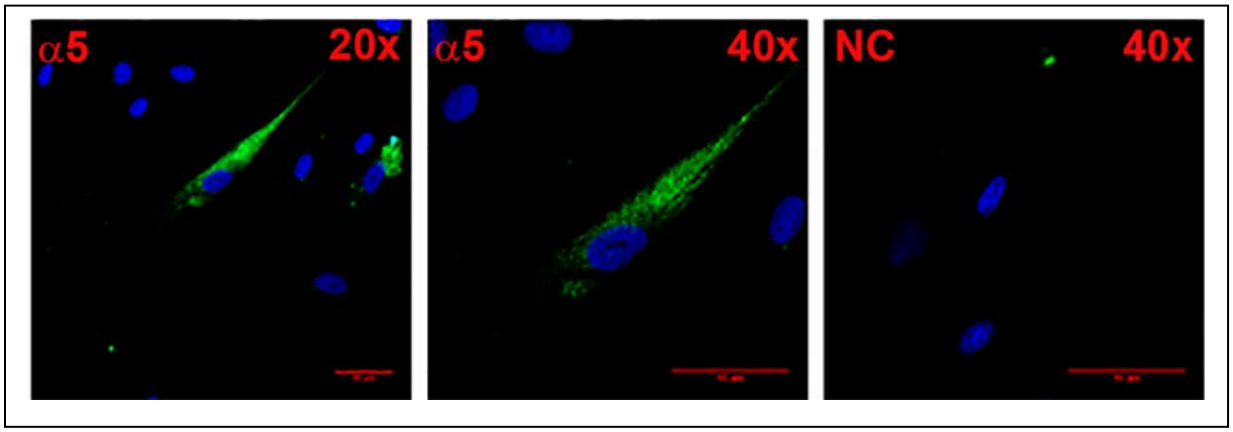

Supplemental Figure 2. Immunofluorescence staining of α5 in HBO cells (43):
Shows immunostaining of α5 HBO cells using 20x and 40x objectives (total 200x and 400x magnification). The panels show merged confocal images of DAPI (blue) and secondary antibody fluorescence (green). The horizontal red lines represent 10 μm.

3

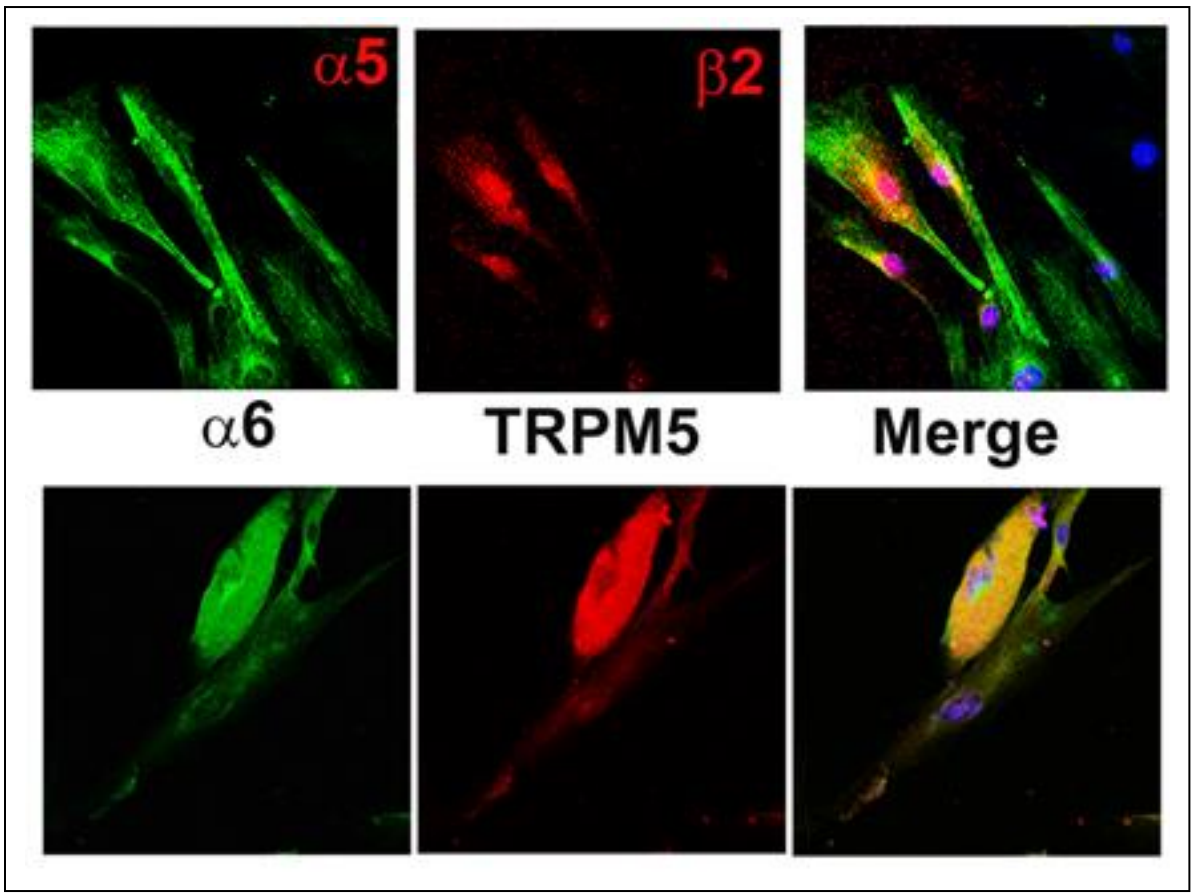

Supplemental Figure 3. Co-localization of α and B subunits in HBO cells and Co-localization of α5 subunit with TRPM5 in HBO cells (43):
Dual immunostaining was used to co-localize α and β subunits in individual HBO cells. Show immunostaining of α5 with β2. The panels show confocal images of α5 (green), β2 (red), DAPI (blue), and merged images of DAPI and dual fluorescence labels. Dual immunostaining was used to co-localize α6 subunit with TRPM5 in individual HBO cells. Show confocal images of α6 (green), TRPM5 (red), DAPI (blue), and merged images of DAPI and dual fluorescence labels.

4

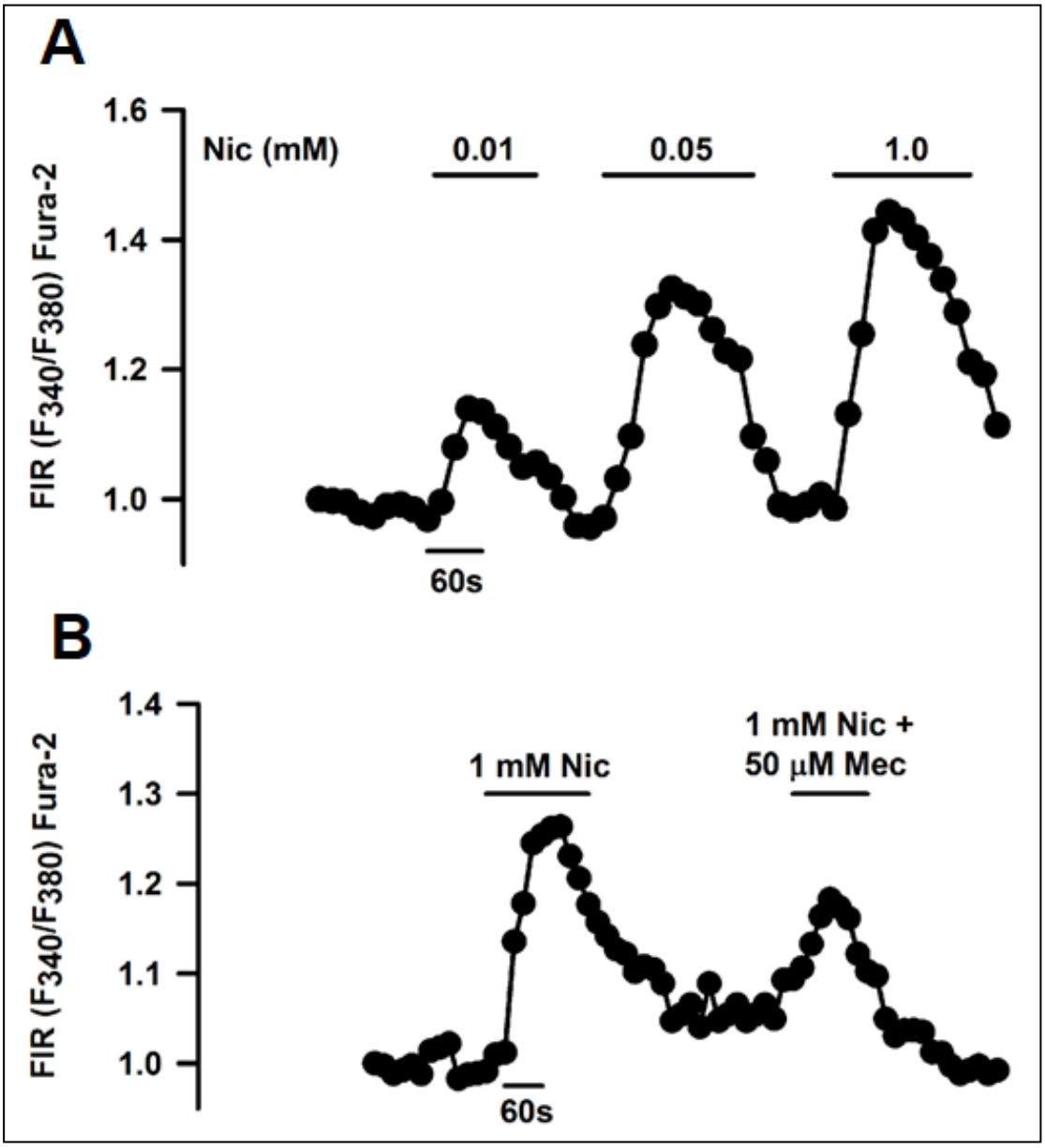

Supplemental Figure 4. Effect of Nicotine and mecamylamine on temporal changes in $[Ca^{2+}]_i$ in individual HBO cells (43):
(A) Shows a representative HBO cell that responded with a dose-dependent increase in FIR when stimulated with 0.01, 0.05 and 1.0 mM Nic. **(B)** Shows another representative HBO cell that responded with an increase in FIR in the presence of 1 mM Nic. Mec (50 μM) inhibited the Nic-induced increase in FIR. In each cell, the FIR was normalized to 1 with respect to its value under the control conditions.

5

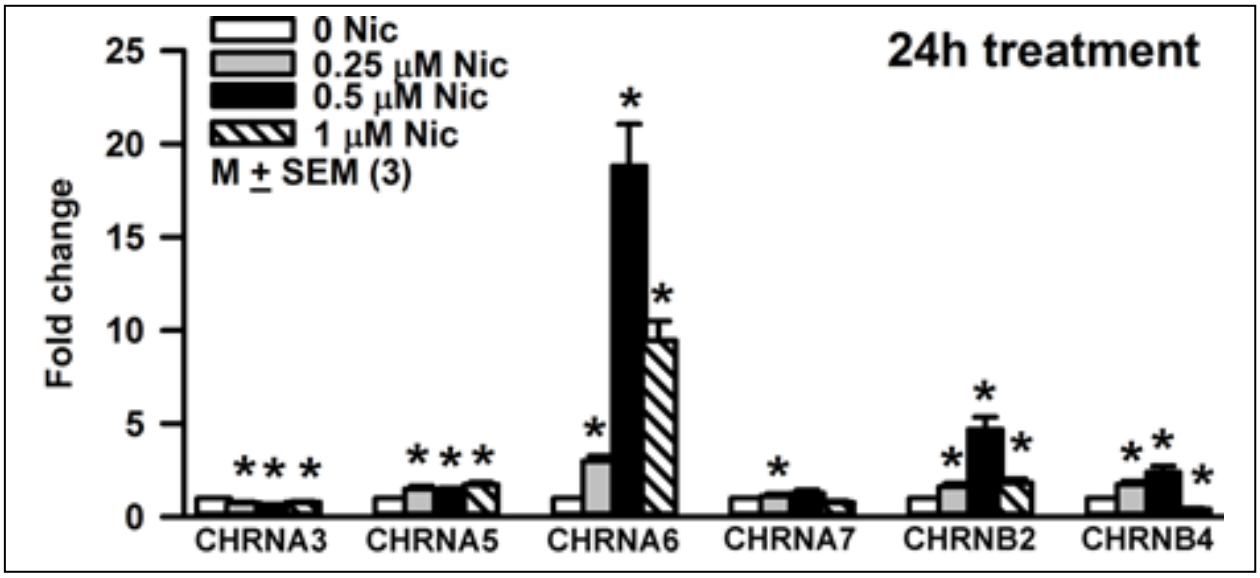

Supplemental Figure 5. Effect of Nic exposure on the nAChR subunit mRNA expression level in HBO cells (43):
After 24h Nic treatment. Relative to control, at 0.25 μM Nic the *p values for α3, α5, A α6, β2, and β4 mRNAs were 0.0111, 0.0306, 0.0017, 0.0239, and 0.0173, respectively. Relative to control, at 0.50 μM Nic the *p values for α3, α5, α6, β2, and β4 mRNAs were 0.0022, 0.0473, 0.0014, 0.0049, and 0.0141, respectively. Relative to control, at 1.0 μM Nic the *p values for α3, α5, α6, β2, and β4 mRNAs were 0.0194, 0.0055, 0.0013, 0.0236, and 0.0003, respectively. Relative to 0.25 μM Nic, at 0.50 μM Nic the *p values for α6 and β 4 were 0.0039 and 0.0024. Relative to 0.50 μM Nic at 1.0 μM Nic the *p values for α6, β, and β4 were 0.0192, 0.0144, and 0.0046, respectively.

6

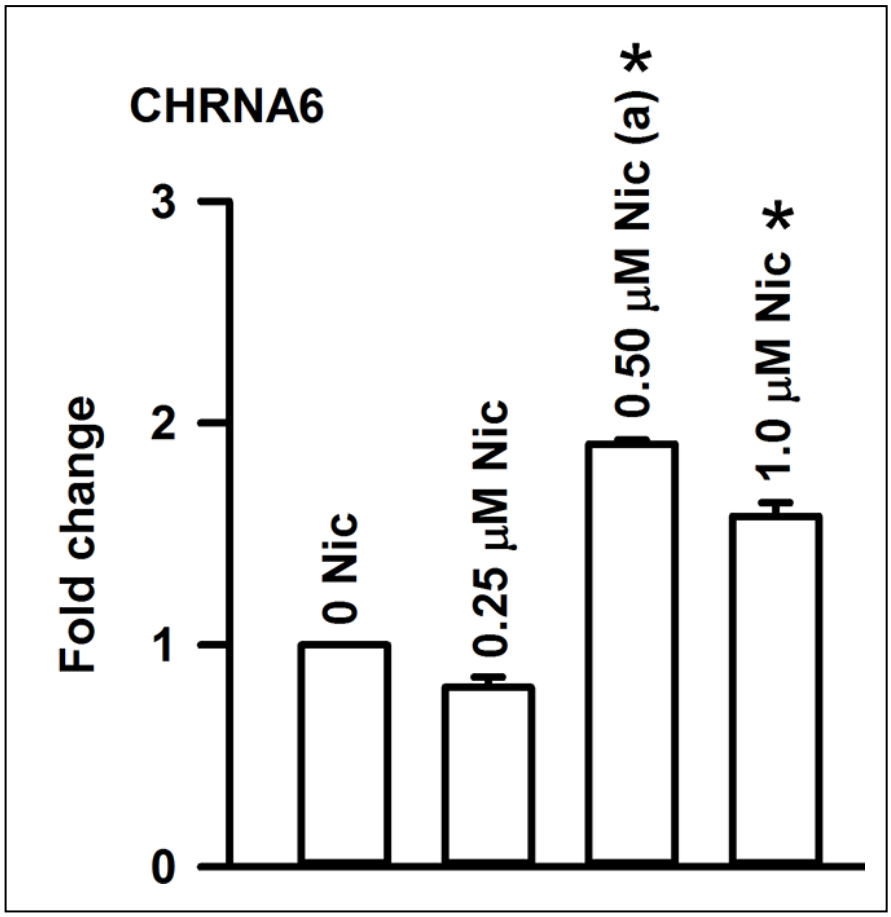

Supplemental Figure 6. Effect of Nicotine and on α6 protein expression in HBO cells (43): HBO cells were treated with Nic (0.25–1.0 μM) for 24h. Western blots were developed using specific α6 antibodies. The fold change in protein expression was calculated with respect to β-actin. The values are means of triplicate measurements.

7

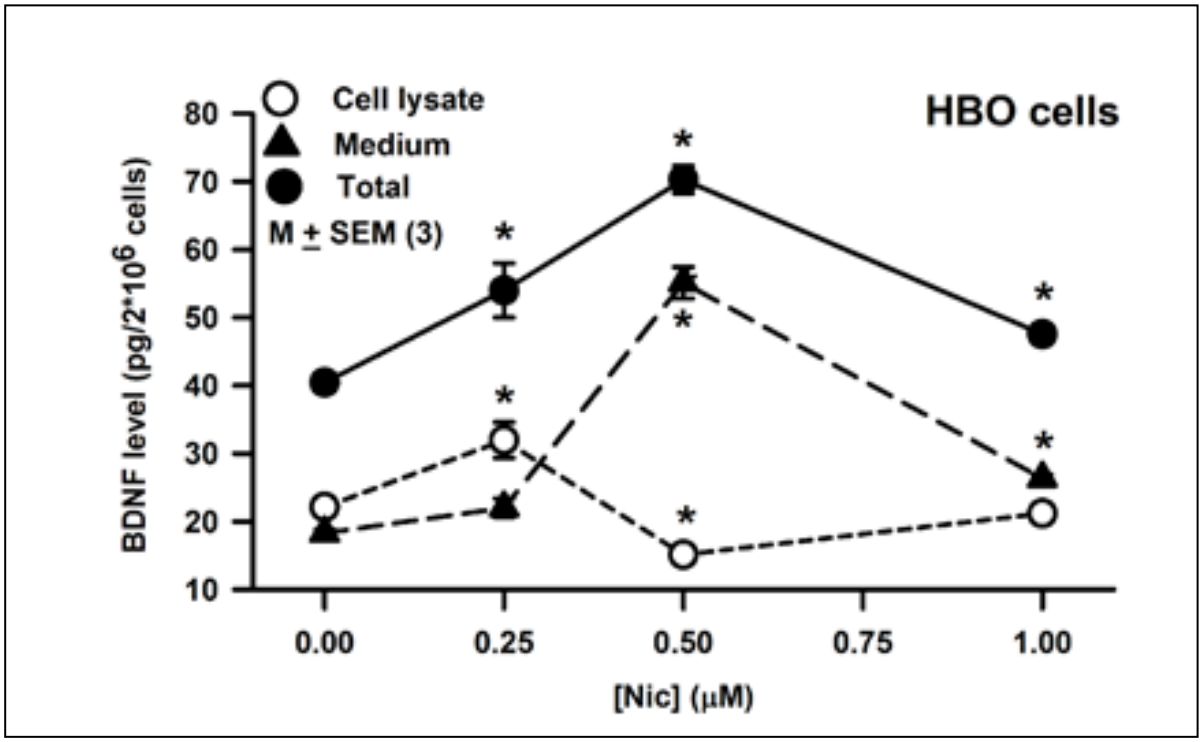

Supplemental Figure 7. Effect of Nicotine on BDNF synthesis and release in HBO cells (43): HBO cells were treated with 0.25, 0.50, and 1.0 μM Nic for 30 min. Following that BDNF concentration was measured in cell lysate and the media. Relative to control BDNF concentration in cell lysate increased at 0.25 μM Nic ($p = 0.0274$) and decreased at 0.5 μM Nic ($p = 0.0055$). No significant increase in BDNF concentration was observed at 0.25 μM Nic, however, at 0.5 μM Nic, BDNF concentration was significantly increased relative to control ($p = 0.0001$). Relative to control at 1.0 μM Nic, a small but significant increase in the BDNF concentration was observed in the media ($p = 0.0004$). The p values for the changes in total BDNF content for 0.25, 0.5 and 1.0 μM Nic were 0.0289, 0.0002, and 0.0014, respectively. The values are mean ± SEM of triplicate measurements

BIBLIOGRAPHY

Bibliography

1. “JUULpod Basics.” JUUL, JUUL Labs, 2018, support.juul.com/home/learn/faqs/juulpod-basics
2. Adil, Aalia E, Meyers A. “Tongue Anatomy.” Overview, Gross Anatomy, Pathophysiologic Variants, MedScape, 20 June 2017, emedicine.medscape.com/article/1899434-overview#a2.
3. Albuquerque EX, Pereira EF, Alkondon M, Rogers SW. Mammalian nicotinic acetylcholine receptors: from structure to function. Physiol Rev. 2009;89(1):73-120.
4. Andresen JH, Løberg EM, Wright M, Goverud IL, Stray-Pedersen B, Saugstad OD. Nicotine affects the expression of brain-derived neurotrophic factor mRNA and protein in the hippocampus of hypoxic newborn piglets. J Perinatal Med. 2009;37:553–560.
5. Benowitz NL, Hukkanen J, Jacob P. Nicotine chemistry, metabolism, kinetics and biomarkers. Handb Exp Pharmacol. 2009;(192):29-60.
6. Lindemann B, Ogiwara Y, Ninomiya Y; The Discovery of Umami, Chemical Senses, Volume 27, Issue 9, 1 November 2002, Pages 843–844, https://doi-org.proxy.library.vcu.edu/10.1093/chemse/27.9.843
7. Blakeslee, Albert F, Salmon TN. “Genetics of Sensory Thresholds: Individual Taste Reactions for Different Substances.” Proceedings of the National Academy of Sciences of the United States of America 21.2 (1935): 84–90. Print.
8. Centers for Disease Control and Prevention (US); National Center for Chronic Disease Prevention and Health Promotion (US); Office on Smoking and Health (US). How Tobacco Smoke Causes Disease: The Biology and Behavioral Basis for Smoking-Attributable Disease: A Report of the Surgeon General. Atlanta (GA): Centers for Disease Control and

Prevention (US); 2010. 4, Nicotine Addiction: Past and Present. Available from: https://www.ncbi.nlm.nih.gov/books/NBK53018/

9. Chandrashekar, Mueller KL, Hoon MA, Adler E, Feng L, Guo W, Zuker CS, Ryba NJ. 2000. T2Rs function as bitter taste receptors. Cell. 100:703–711. doi:10.1016/S0092-8674(00)80706-0
10. Chan, RB, Waters H, Lima ER (2010). A proton current drives action potentials in genetically identified sour taste cells. Proceedings of the …, 107(51), 22320–5. https://doi.org/10.1073/pnas.1013664107
11. Chaudhari N, Roper SD (2010). The cell biology of taste. Journal of Cell Biology. https://doi.org/10.1083/jcb.201003144
12. Cohen N. (2017).The genetics of the bitter taste receptor T2R38 in upper airway innate immunity and implications for chronic rhinosinusitis. Laryngoscope. 2016;127(1):44-51.
13. Cuenca L. (2013). The Bittersweet Truth of Sweet and Bitter Taste Receptors. [Blog] Science in the News. Available at: http://sitn.hms.harvard.edu/flash/2013/the-bittersweet-truth-of-sweet-and-bitter-taste-receptors
14. DeSimone JA, Beauchamp G, Drewnowski A, Johnson G; Sodium in the food supply: challenges and opportunities, Nutrition Reviews, Volume 71, Issue 1, 1 January 2013, Pages 52–59, https://doi.org/10.1111/nure.12006
15. DeSimone JA, Lyall V. Taste receptors in the gastrointestinal tract III. Salty and sour taste: Sensing of sodium and protons by the tongue. American Journal of Physiology—Gastrointestinal and Liver Physiology. 2006;291(6):G1005–G1010.

16. Devesa, Isabel, et al. "αCGRP is essential for algesic exocytotic mobilization of TRPV1 channels in peptidergic nociceptors." Proceedings of the National Academy of Sciences 111.51 (2014): 18345-18350.

17. Dewis ML, et al. "N-geranyl cyclopropyl-carboximide modulates salty and umami taste in humans and animal models." Journal of neurophysiology 109.4 (2012): 1078-1090.

18. Doty RL (2012). Gustation. Wiley Interdisciplinary Reviews: Cognitive Science. https://doi.org/10.1002/wcs.156

19. Roura E, Aldayyani A, Thavaraj P, Prakash S, Greenway D, Thomas WG, Meyerhof W, Roudnitzky N, Foster SR. Variability in Human Bitter Taste Sensitivity to Chemically Diverse Compounds Can Be Accounted for by Differential TAS2R Activation, Chemical Senses, Volume 40, Issue 6, 1 July 2015, Pages 427–435, https://doi.org/10.1093/chemse/bjv024

20. Finger TE, et al. "ATP signaling is crucial for communication from taste buds to gustatory nerves." Science 310.5753 (2005): 1495-1499.

21. Gravina SA, Yep GL, Khan M. Human biology of taste. Ann Saudi Med. 2013;33:217–222. https://www.ncbi.nlm.nih.gov/pubmed/23793421

22. Hamm, Lee L, Feng Z, Hering-Smith KS. "Regulation of sodium transport by ENaC in the kidney." Current opinion in nephrology and hypertension 19.1 (2010): 98.

23. He W, Yasumatsu K, Varadarajan V, Yamada A, Lem J, Ninomiya Y, Damak S. (2004). Umami taste responses are mediated by alpha-transducin and alpha-gustducin. The Journal of Neuroscience : The Official Journal of the Society for Neuroscience, 24(35), 7674–80. https://doi.org/10.1523/JNEUROSCI.2441-04.2004

24. Henney JE, Taylor CL, Boon CS. "Taste and flavor roles of sodium in foods: A unique challenge to reducing sodium intake." Strategies to Reduce Sodium Intake in The United States; National Academies Press: Washington, DC, USA (2010).
25. Hochheimer, Andreas, et al. "Endogenous gustatory responses and gene expression profile of stably proliferating human taste cells isolated from fungiform papillae." Chemical senses 39.4 (2014): 359-377.
26. Huang, Angela L, et al. "The cells and logic for mammalian sour taste detection." Nature 442.7105 (2006): 934.
27. Kinnamon SC. (1993). Role of apical ion channels in sour taste transduction. Ciba Found Symp, 1799422191, 201–210.
28. Kinnamon SC. (2009). Umami taste transduction mechanisms. In American Journal of Clinical Nutrition (Vol. 90). https://doi.org/10.3945/ajcn.2009.27462K
29. Kobayashi Y, Habara M, Ikezazki H, Chen R, Naito Y, Toko K. (2010). Advanced taste sensors based on artificial lipids with global selectivity to basic taste qualities and high correlation to sensory scores. Sensors. https://doi.org/10.3390/s100403411
30. Lee RJ, Cohen NA. Taste receptors in innate immunity. Cell Mol Life Sci. 2015;72(2):217–36. pmid:25323130; PubMed Central PMCID: PMCPMC4286424.
31. Li X, Staszewski L, Xu H, Durick K, Zoller M, & Adler E. (2002). Human receptors for sweet and umami taste. Proc Natl Acad Sci U S A, 99(7), 4692–4696. https://doi.org/10.1073/pnas.072090199
32. Lindemann B. (2001). Receptors and transduction in taste. Nature, 413(6852), 219– 225. https://doi.org/10.1038/35093032

33. Lyall V, Alam RI, Phan TH, Phan DQ, Heck GL, & DeSimone JA (2002). Excitation and adaptation in the detection of hydrogen ions by taste receptor cells: a role for cAMP and ca(2+). J Neurophysiol, 87(1), 399–408.

34. Lyall V, et al. "The mammalian amiloride-insensitive non-specific salt taste receptor is a vanilloid receptor-1 variant." The Journal of physiology 558.1 (2004): 147-159.

35. Margolskee RF (2002). Molecular mechanisms of bitter and sweet taste transduction. Journal of Biological Chemistry, 277(1), 1–4. https://doi.org/10.1074/jbc.R100054200

36. Mishra A, Chaturvedi P, Datta S, Sinukumar S, Joshi P, Garg A. Harmful effects of nicotine. Indian J Med Paediatr Oncol. 2015;36(1):24-31.

37. Mistretta CM, Kumari A. (2017). Tongue and Taste Organ Biology and Function: Homeostasis Maintained by Hedgehog Signaling. Annual Review of Physiology, 79(1), 335–356. https://doi.org/10.1146/annurev-physiol-022516-034202

38. Montmayeur JP, & Matsunami H (2002). Receptors for bitter and sweet taste Jean-Pierre Montmayeur * and Hiroaki Matsunami, 366–371

39. Neta ERDC., Johanningsmeier SD, McFeeters RF (2007). The chemistry and physiology of sour taste - A review. Journal of Food Science, 72(2). https://doi.org/10.1111/j.1750-3841.2007.00282.x

40. Oliveira-Maia AJ, Stapleton-Kotloski JR, Lyall V, et al. Nicotine activates TRPM5-dependent and independent taste pathways. Proc Natl Acad Sci U S A. 2009;106(5):1596-601.

41. Ozdener, Hakan, Spielman AI, and Rawson NE. "Isolation and culture of human fungiform taste papillae cells." Journal of visualized experiments: JoVE 63 (2012).

42. Pandya A, Yakel JL. Allosteric modulators of the α4β2 subtype of neuronal nicotinic acetylcholine receptors. Biochem Pharmacol. 2011;82(8):952-8.

43. Qian J, Mummalaneni S, Larsen J, Grider JR, Spielman AI, Özdener MH, et al. (2018) Nicotinic acetylcholine receptor (CHRN) expression and function in cultured human adult fungiform (HBO) taste cells. PLoS ONE 13(3): e0194089. https://doi.org/10.1371/journal.pone.0194089

44. Ruiz, Collin, et al. "Detection of NaCl and KCl in TRPV1 knockout mice." Chemical senses 31.9 (2006): 813-820.

45. Saha SP, Bhalla DK, Whayne TF, Gairola C. Cigarette smoke and adverse health effects: An overview of research trends and future needs. Int J Angiol. 2007;16(3):77-83.

46. Sassone-Corsi, P. (2012). The Cyclic AMP pathway. Cold Spring Harbor Perspectives in Biology, 4(12). https://doi.org/10.1101/cshperspect.a011148

47. Smith DV, Margolskee RF (2001). Making sense of taste. Scientific American, 284(3), 32–39. https://doi.org/10.1038/scientificamerican0906-84sp

48. Spielman AI (1998). Gustducin and its role in taste. Journal of Dental Research, 77(4), 539–544. https://doi.org/10.1177/00220345980770040601

49. Stone LM, Finger TE, Tam PP, Tan SS (1995). Taste receptor cells arise from local epithelium, not neurogenic ectoderm. Proceedings of the National Academy of Sciences of the United States of America, 92(March), 1916–1920. https://doi.org/10.1073/pnas.92.6.1916

50. Veerkar, Sanjay. “Side-Effects of Nicotine.” ECig Lounge, Magic Mist, 19 Apr. 2012, eciglounge.themagicmist.com/side-effects-of-nicotine/.

51. Yarmolinsky DA, Zuker CS, Ryba NJP. "Common sense about taste: from mammals to insects." Cell 139.2 (2009): 234-244.

52. Zhang Y, Hoon MA, Chandrashekar J, Mueller KL, Cook, B, Wu, Ryba NJP (2003). Coding of sweet, bitter, and umami tastes: Different receptor cells sharing similar signaling pathways. Cell, 112(3), 293–301.

53. Zhao, Grace Q, et al. "The receptors for mammalian sweet and umami taste." Cell 115.3 (2003): 255-266.

54. Govind AP, Walsh H, Green WN. Nicotine-induced upregulation of native neuronal nicotinic receptors is caused by multiple mechanisms. *J Neurosci*. 2012;32(6):2227-38.

55. Russell MA, Wilson C, Patel UA, Feyerabend C, Cole PV. Plasma nicotine levels after smoking cigarettes with high, medium, and low nicotine yields. Br Med J. 1975;2(5968):414-6.

56. Eguchi K, Ohtubo Y, Yoshii K. Functional expression of M3, a muscarinic acetylcholine receptor subtype, in taste bud cells of mouse fungiform papillae. Chem Senses. 2008;33:47–55. doi: 10.1093/chemse/bjm065

57. Ogura T, Lin W. Acetylcholine and Acetylcholine Receptors in Taste Receptor Cells, *Chemical Senses*, Volume 30, Issue suppl_1, 1 January 2005, Pages i41, https://doi.org/10.1093/chemse/bjh103

58. Ren ZJ, Mummalaneni S, Qian J, Baumgarten CM, DeSimone JA, Lyall V (2015) Nicotinic Acetylcholine Receptor (nAChR) Dependent Chorda Tympani Taste Nerve Responses to Nicotine, Ethanol and Acetylcholine. PLoS ONE 10(6): e0127936. https://doi-org.proxy.library.vcu.edu/10.1371/journal.pone.0127936

59. Qian J, Mummalaneni S, Grider JR, Damaj MI, Lyall V (2018) Nicotinic acetylcholine receptors (nAChRs) are expressed in Trpm5 positive taste receptor cells (TRCs). PLoS ONE 13(1): e0190465.
https://doi-org.proxy.library.vcu.edu/10.1371/journal.pone.0190465

60. Kalamida D, Poulas K, Avramopoulou V, Fostieri E, Lagoumintzis G, Lazaridis K, Sideri A, Zouridakis M, Tzartos SJ. Muscle and neuronal nicotinic acetylcholine receptors. Structure, function and pathogenicity. FEBS J 274: 3799–845, 2007.

61. Wang Y, Pereira EF, Maus AD, Ostlie NS, Navaneetham D, Lei S, Albuquerque EX & Conti-Fine BM (2001) Human bronchial epithelial and endothelial cells express alpha7 nicotinic acetylcholine receptors. Mol Pharmacol 60, 1201–1209.

62. Tournier JM, Maouche K, Coraux C, Zahm JM, Cloez-Tayarani I, Nawrocki-Raby B, Bonnomet A, Burlet H, Lebargy F, Polette M et al. (2006) alpha3alpha5beta2-Nicotinic acetylcholine receptor contributes to the wound repair of the respiratory epithelium by modulating intracellular calcium in migrating cells. Am J Pathol 168, 55–68.

63. Chernyavsky AI, Arredondo J, Marubio LM & Grando SA (2004) Differential regulation of keratinocyte chemokinesis and chemotaxis through distinct nicotinic receptor subtypes. J Cell Sci 117, 5665–5679.

64. Zhang J, Xiao Y, Abdrakhmanova G, Wang W, Cleemann L, Kellar KJ, Morad M. Activation and Ca2+ permeation of stably transfected alpha3/beta4 neuronal nicotinic acetylcholine receptor. Mol Pharmacol. 1999;55:970–981.

65. Mesnard-Rouiller L, Bismith J, Wakkach A, Poea-Guyon S & Berrih-Aknin S (2004) Thymic myoid cells express high levels of muscle genes. J Neuroimmunol 148, 97–105.

66. Levinson AI, Song D, Gaulton G & Zheng Y (2004) The intrathymic pathogenesis of myasthenia gravis. Clin Dev Immunol 11, 215–220.

67. Colombara M, Antonini V, Riviera AP, Mainiero F, Strippoli R, Merola M, Fracasso G, Poffe O, Brutti N, Tridente G et al. (2005) Constitutive activation of p38 and ERK1/2 MAPKs in epithelial cells of myasthenic thymus leads to IL-6 and RANTES overexpression: effects on survival and migration of peripheral T and B cells. J Immunol 175, 7021–7028.

68. Inoue M, Okumura M, Miyoshi S, Shiono H, Fukuhara K, Kadota Y, Shirakura R & Matsuda H (1999) Impaired expression of MHC class II molecules in response to interferon-gamma (IFN-gamma) on human thymoma neoplastic epithelial cells. Clin Exp Immunol 117, 1–7

69. Mandl P, Kiss JP. Role of presynaptic nicotinic acetylcholine receptors in the regulation of gastrointestinal motility. Brain Res Bull 72: 194–200, 2007.

70. Zdanowski R, Krzyżowska M, Ujazdowska D, Lewicka A, Lewicki S. Role of α7 nicotinic receptor in the immune system and intracellular signaling pathways. Cent Eur J Immunol. 2015;40(3):373-9.

71. Olofsson PS, Katz DA, Rosas-Ballina M, et al. α7 nicotinic acetylcholine receptor (α7nAChR) expression in bone marrow-derived non-T cells is required for the inflammatory reflex. Mol Med. 2012;18:539–543.

72. Wang H, Yu M, Ochani M, et al. Nicotinic acetylcholine receptor _7 subunit is an essential regulator of inflammation. Nature. 2003;421:384–388.

73. Rezonzew G, Chumley P, Feng W et al. Nicotine exposure and the progression of chronic kidney disease: role of the alpha7-nicotinic acetylcholine receptor. Am J Physiol Renal Physiol 2012; 303: F304–F312

74. Jain G, Jaimes EA. Nicotine signaling and progression of chronic kidney disease in smokers. Biochem Pharmacol. 2013;86(8):1215-23.

75. Jaimes EA, Tian RX, Raij L. Nicotine: the link between cigarette smoking and the progression of renal injury? Am J Physiol Heart Circ Physiol. 2007;292:H76–82

76. Qian J, Mummalaneni SK, Alkahtani RM, et al. Nicotine-Induced Effects on Nicotinic Acetylcholine Receptors (nAChRs), Ca2+ and Brain-Derived Neurotrophic Factor (BDNF) in STC-1 Cells. PLoS One. 2016;11(11):e0166565. Published 2016 Nov 15. doi:10.1371/journal.pone.0166565

77. Arredondo J, Hall LL, Ndoye A, Nguyen VT, Chernyavsky AI, Bercovich D, et al. Central role of fibroblast alpha3 nicotinic acetylcholine receptor in mediating cutaneous effects of nicotine. Lab Invest. 2003; 83:207–25. pmid:12594236

78. Brown KC, Perry HE, Lau JK, Jones DV, Pulliam JF, Thornhill BA, et al. Nicotine induces the up-regulation of the α7-nicotinic receptor (α7-nAChR) in human squamous cell lung cancer cells via the Sp1/GATA protein pathway. J Biol Chem. 2013; 288:33049–33059. pmid:24089524

79. Neural plasticity in the gustatory system. Nutr Rev. 2004;62(11 Pt 2):S208-17; discussion S224-41

80. Qian J, Mummalaneni S, Alkahtani RM, Mahavadi S, Murthy KS, Grider JR, e al. Nicotine-Induced Effects on Nicotinic Acetylcholine Receptors (nAChRs), Ca2+ and Brain-Derived

Neurotrophic Factor (BDNF) in STC-1 Cells. PLoS One. 2016; 11: e0166565. pmid:27846263

81. Thomas P, Smart TG. HEK293 cell line: A vehicle for the expression of recombinant proteins. Journal of Pharmacological and Toxicological Methods. 2005; 51:187–200. pmid:15862464

Vita

James Larsen was born on December 13th, 1991 in Virginia Beach, Virginia. He was raised in Gainesville, Virginia and graduated from Battlefield High School in Haymarket, Virginia. He received his Bachelor of Arts from the University of Virginia, Charlottesville, Virginia in May 2014. He will receive his Master of Science in Physiology & Biophysics from Virginia Commonwealth University in December 2018.